A Method for Finding Galaxy Groups in Early Formation Stages Applied to RESOLVE and ECO

By
Ella Castelloe

Senior Honors Thesis
Department of Physics and Astronomy
University of North Carolina at Chapel Hill

May 5, 2021

Approved:

Sheila Kannappan, Thesis Advisor

Adrienne Erickcek, Reader

Louise Dolan, Reader

Draft version May 5, 2021
Typeset using LaTeX **twocolumn** style in AASTeX63

A Method For Finding Galaxy Groups in Early Formation Stages Applied to RESOLVE and ECO

Ella R. Castelloe
Advisor: Sheila J. Kannappan

ABSTRACT

The most common galaxy group finding algorithm, Friends-of-Friends (FoF), finds "settled" groups that share a common dark matter halo but misses groups that are in earlier stages of formation and have not yet merged halos. We present a new algorithm that is designed to find groups like the Local Group that are gravitationally bound but do not yet share a common halo and are not identified as FoF groups. We use escape velocity to test whether settled groups are bound to other nearby settled groups (including "groups" of one solitary galaxy). We statistically correct for projection effects present in observational data using mock catalogs containing simulated three-dimensional data. We apply the boundness method to RESOLVE and ECO, two large volume-limited surveys of galaxies in the local Universe. Using our boundness method increases the number of multiple galaxy systems that are identified and decreases the number of single galaxy systems. We find evidence that the bound systems we identify are truly groups in the early stages of formation, based on comparisons of large scale environment and virialization state with settled groups. We identify "Local Group analogues" that are similar to the real Local Group. We find 32 Local Group analogues in RESOLVE and 229 in ECO. In RESOLVE and ECO, about 13% of all multiple-galaxy systems are Local Group analogues and about 8% of all galaxies belong to a Local Group analogue. Local Group analogues are among the most virialized systems found by the boundness method in RESOLVE and ECO, with a median crossing time about three times shorter than other bound multi-group systems with similar masses. To determine how well the boundness method finds systems like the Local Group, we identify a population of Local Group analogues in the mock catalogs. FoF finds only 6% of the Local Group analogues, whereas the boundness method finds 97%. We compare properties of different categories of bound systems in RESOLVE and ECO, focusing on their evolutionary connection, and find that gas content may be higher in small settled groups (FoF groups with halo mass $< 10^{12} M_{\odot}$) than in proto-groups (bound multi-group systems with system mass $< 10^{12} M_{\odot}$) at fixed virialization state.

1. INTRODUCTION

The Milky Way and Andromeda, two giant galaxies in the Local Group, currently reside in separate dark matter halos (Cox & Loeb 2008). Over the course of the next several billion years, the halos of the Milky Way and Andromeda will merge (van der Marel et al. 2012) and the Local Group will become a "settled group" that shares a single dark matter halo. Most group finders are designed to find settled groups and do not find groups like the Local Group. In this paper we present a group finder that finds systems like the Local Group that are not yet fully settled by testing for gravitational boundness between neighboring settled groups (including solitary galaxies, which we call "$N = 1$ groups"). This group finder allows us to study how the properties of galaxy groups change as groups evolve, and to identify and study other groups like our own in the Universe.

In order to study galaxy groups in different stages of formation, including Local Group (LG) analogues, we need to be able to identify both groups in the early stages of formation and settled groups. Friends-of-Friends (FoF) is a commonly used group finder that can be calibrated, as in Duarte & Mamon (2014) and Berlind et al. (2006), to find settled groups. The algorithm groups galaxies based on proximity using linking lengths in the on-sky and line-of-sight directions to join galaxies into groups if they are near enough (Huchra & Geller 1982). FoF is widely used because it is relatively simple and recovers groups in a single shared halo fairly well (Old et al. 2014), although it does tend to overestimate membership in small groups and underestimate membership in large groups (Stothert et al. 2019).

While FoF does sometimes mistakenly join together nearby small groups that do not share a common halo, it is not designed to find groups like the Local Group that are gravitationally bound but do not yet share a common dark matter halo. To study groups in the early stages of formation, we must depend on other group finders. Kourkchi & Tully (2017) identified galaxy "as-

sociations" consisting of galaxies within a sphere of high enough density to have decoupled from cosmic expansion but not close enough to have fully settled. Tempel et al. (2017) identified potentially merging groups by searching for neighboring settled groups whose group centers were closer than the sum of the two groups' virial radii. Their criteria for classifying merging groups were fairly restrictive, and they classified only about 0.6% of groups with more than two members as potentially merging. Leong & Saslaw (2004) used simulations to predict how common groups like the Local Group are, and predicted that at least 10% of galaxies belong to a loosely clustered group like the Local Group that is gravitationally bound but not virialized.

We present a new algorithm that finds groups in the early stages of formation by testing for gravitational boundness between neighboring settled groups (including $N = 1$ groups). Our algorithm finds bound multi-group systems that, like the associations in Kourkchi & Tully (2017) and the potentially merging groups in Tempel et al. (2017), consist of multiple dark matter halos that are likely to merge into a single halo over time. Our boundness criterion does not necessarily require that neighboring groups be close enough for their radii to overlap, making our algorithm inclusive of more groups in the early stages of formation than the method of Tempel et al. (2017). Our algorithm should find a population similar to the associations of Kourkchi & Tully (2017), although their method for finding associations does not explicitly test for gravitational boundness.

Previous work has found that groups in the early stages of formation exhibit different evolutionary and virialization state metrics compared to settled groups. Rood & Dickel (1978) and Ferguson & Sandage (1990) classify samples of galaxy groups as gravitationally bound based on their velocity dispersions and group crossing times, which are both measures of virialization state. They both find that all of the galaxy groups in their samples (92 groups in Rood & Dickel 1978 and five groups in Ferguson & Sandage 1990) are gravitationally bound based on these metrics. Firth et al. (2006) use these same metrics, and also include measures of compactness and substructure (Dressler & Shectman 1988) to classify groups as "loose" or "compact," finding that in their sample of six groups, three were loose and three were compact. We will expand on these studies of evolutionary and virialization state metrics using a large, complete sample of groups that is representative of the local Universe. Our new method enables the comparison of evolutionary and virialization state metrics, as well as galaxy and group properties, between settled groups and groups in the early stages of formation.

Identifying groups in the early stages of formation allows for the identification of Local Group (LG) analogues, which can be used to study how groups like our own compare to other types of groups in the Universe. LG analogues consist of two giant galaxies, analogues for the Milky Way (MW) and Andromeda (M31), and their satellites. There are four criteria used to identify LG analogues in simulations: the masses, separation, and relative radial velocity of the two giant galaxies, and the isolation of the LG analogue from other nearby giant galaxies (Fattahi et al. 2016; Zhai et al. 2020; Carlesi et al. 2019; Li & White 2008; Garrison-Kimmel et al. 2019). Our new method enables the identification and study of LG analogues, providing context on how common a group environment like that of the Milky Way is in the Universe.

The group environment in which a galaxy resides affects the galaxy's properties and evolution by regulating the amount of gas available for star formation, making the identification and study of groups vital for a full understanding of galaxy evolution. There are several important halo mass scales that mark transitions in the availability of cold gas that galaxies use to form stars. Below the "gas-richness threshold" scale at a halo mass of about $10^{11.5}$ $M_\odot$, cold flows of gas supply galaxies with fuel for star formation (Kannappan et al. 2013). Theoretical studies (e.g., Dekel & Birnboim 2006) predict shock heating of halo gas to the virial temperature of the halo starting in the center of the halo at the gas-richness threshold scale and continuing out to the virial radius by the "bimodality" halo mass scale of about 10^{12} $M_\odot$. The halo mass range between the gas-richness threshold scale and the bimodality scale represent a key transition in the mode of gas accretion that affects galaxy evolution by halting cold flows of gas that would fuel star formation.

Interactions within groups also play an important role in regulating the amount of gas available for star formation. Galaxies in halos with mass above about 10^{12} $M_\odot$are subject to removal of gas by ram pressure stripping (Gunn 1972; Abadi et al. 1999; Spekkens et al. 2014). Tidal interactions between galaxies in a group can take many forms that can lead to gas being removed from or accreted onto galaxies (Rasmussen et al. 2012; Larson et al. 1980; Joseph & Wright 1985). The importance of group environment, and especially group halo mass, in determining the gas content of galaxies motivates our study of groups in the early stages of formation that do not yet share a common dark matter halo.

Section 2 describes the data sets we used and why they are suitable for group finding work. Section 3 details how our method tests for gravitational boundness,

and how we correct for projection effects that arise from using observational data with projected quantities. Section 4 discusses evidence bearing on whether the bound multi-group systems we identify really are groups in the early stages of formation, and includes comparisons of evolutionary and virialization state metrics. We also identify and study a population of Local Group analogues. Section 5 compares our catalog of bound multi-group systems to previous work. Section 6 summarizes our conclusions.

2. DATA

2.1. *RESOLVE and ECO*

The REsolved Spectroscopy of a Local VolumE (RESOLVE, Kannappan & Wei 2008) and the Environmental COntext Catalog (ECO, Moffett et al. 2015) are two highly-complete, volume-limited surveys of the local Universe. Volume-limited surveys that are complete down to an absolute magnitude floor within the survey volume are ideal for identifying and studying galaxy groups because they eliminate selection bias towards bright, massive galaxies, allowing us to identify samples of groups that accurately reflect the real population of groups in the Universe. We can also use volume-limited surveys to study large scale structure in the cosmic web by looking at group properties as a function of environment without relying on statistical completeness corrections. RESOLVE and ECO are both complete down to the gas-rich dwarf galaxy regime, enabling statistically unbiased studies of small groups that would be impossible in a flux-limited survey.

RESOLVE contains >1500 galaxies in two equatorial footprints (the A-semester with RA from 8.75-15.75 hr, Dec from 0 to +5 degrees and the B-semester with RA from 22-3 hr, Dec -1.25 to +1.25 degrees) at redshifts between 4500 - 7000 km s^{-1}, encompassing a total volume of $\sim$52,000 Mpc^3. RESOLVE-A is complete down to an r-band absolute magnitude $M_r = -17.33$ mag floor, and is complete down to a baryonic (stellar + atomic gas) mass of approximately $10^{9.3}$ $M_\odot$. RESOLVE-B overlaps with the deeply imaged SDSS Stripe-82 region, and is thus complete to a slightly dimmer absolute magnitude floor of $M_r = -17$, and a baryonic mass completeness limit of approximately $10^{9.1}$ $M_\odot$(Eckert et al. 2016). RESOLVE has a complete HI gas census (Stark et al. 2016), enabling a reliable study of the gas content of the groups we identify.

ECO is an archival survey that encompasses RESOLVE-A in an approximately 10 times larger volume, providing a large dataset ideal for studies of large-scale environment and for calibration of cosmic variance. ECO is less complete than RESOLVE, with a magnitude floor of $M_r = -17.33$, and combines HI observations from the RESOLVE-A and ALFALFA-40 surveys, relying on photometric gas fractions to estimate gas masses for galaxies with no observations (Eckert et al. 2015). We also use additional HI data from a new cross-match by Zackary Hutchens with ALFALFA-100 to increase the number of HI observations for our gas content analysis. ECO contains approximately 10,000 galaxies at redshifts between 3000 - 7000 km s^{-1} within a survey volume of $\sim$600,000 Mpc^3.

RESOLVE and ECO both contain a redshift buffer of 470 km s^{-1} to mitigate edge effects in group finding and environmental metrics. Settled group membership in RESOLVE and ECO is determined with FoF (Eckert et al. 2017). Halo Abundance Matching (HAM, Blanton & Berlind 2007) is used to estimate halo masses of settled groups from group-integrated luminosity, assuming zero scatter in the relation between a group's halo mass and total luminosity (Eckert et al. 2016). Unless otherwise noted, we use a combined sample of ECO and RESOLVE-B for our analyses.

2.2. *Mock Catalog*

We use mock catalogs of galaxies to test and calibrate our method using simulated three-dimensional information of dark matter, distances, and peculiar velocities. Our mock catalogs were created by A. Berlind, V. Calderon, and M. Asad. The mocks are built on an N-body simulation, similar to simulations used in Moffett et al. (2015) and Stark et al. (2016) but with some modifications that will be described in a future work. Galaxies are populated into dark matter halos to match the conditional luminosity function of ECO. Mock catalogs with the same volume and shape as ECO are created by defining subvolumes relative to a hypothetical observer. The galaxies are assigned observed quantities such as RA, declination, and redshift so that the mock catalogs contain both three-dimensional information as well as two-dimensional projected quantities that mimic what we would observe.

We consider a "true group" to be a group of galaxies known to share a common dark matter halo in the simulation with a corresponding true halo mass determined by summing up the dark matter mass within the halo volume in the simulation. To construct observational FoF groups from the mocks, we perform FoF group finding, matching the original linking lengths used for ECO in Eckert et al. (2016). FoF attempts to recover the true halo groups but does so imperfectly. Halo masses are assigned to FoF groups using HAM. We use the mock catalogs to statistically correct the projection effects that arise from applying our boundness method to

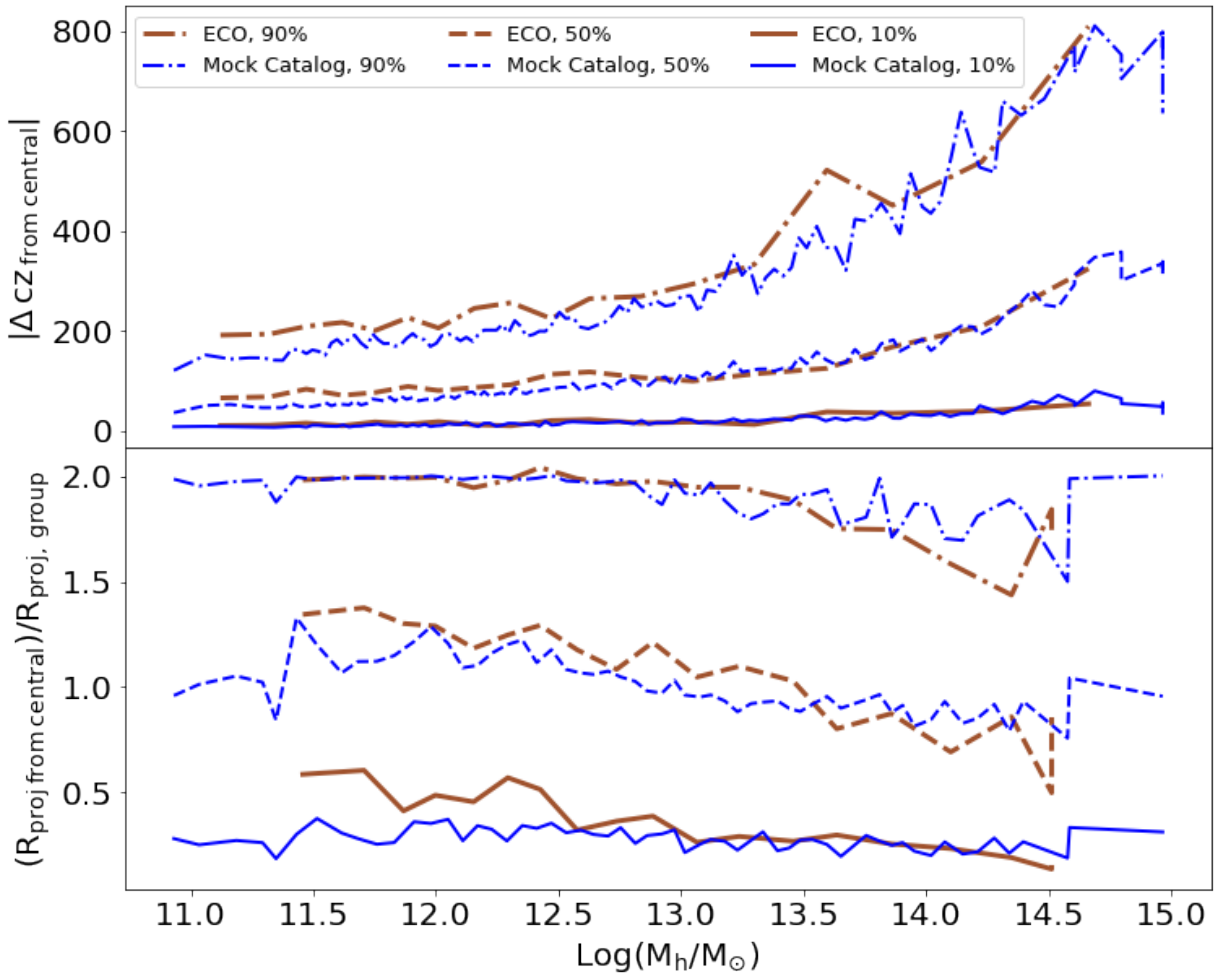

Figure 1: Conditional probability plots showing, for every FoF group in ECO and the mock catalogs as a function of HAM halo mass: (top) the distribution of relative velocity between the group central (galaxy with brightest absolute r-band magnitude) and each satellite in the group and (bottom) the distribution of radial projected distance from group central to each satellite in the group, with 10th, 50th, and 90th percentile relative velocities and distances in each halo mass bin marked. Both the radial and relative velocity distributions are very similar between ECO and the mock catalog.

real data, so it is important that the group finding in the mock catalogs function similarly to group finding in real data. Because the mock catalogs have the same dimensions and conditional luminosity function as ECO, we can define a magnitude floor of $M_r = -17.33$ to create a volume-limited survey with completeness similar to ECO. Figure 1 shows that the radial and velocity distributions of satellites within FoF groups in ECO and in the mock catalogs are similar.

3. METHODS

3.1. *The Boundness Method*

3.1.1. *Description of the Boundness Method*

The boundness method requires a catalog of settled groups (groups that share a common dark matter halo) identified with a method such as FoF. Each settled group in the group catalog, including $N = 1$ groups, is tested for gravitational boundness to its nearest neighbor settled group. For the purpose of testing for gravitational boundness, each settled group is treated as a point particle located at the arithmetic group center (the RA, Dec, and redshift coordinates of a group center are the mean RA, Dec, and redshift of all group members). For a given settled group (the "chosen group"), we use a K-D Tree nearest neighbor search (Bentley 1975) to find the closest settled group in the survey (the "neighbor group"). We calculate the escape velocity from the chosen group at the location of the neighbor group, given by

$$v_{\rm escape} = \sqrt{\frac{2GM}{R_{\rm grp-grp\ (3D)}}}, \qquad (1)$$

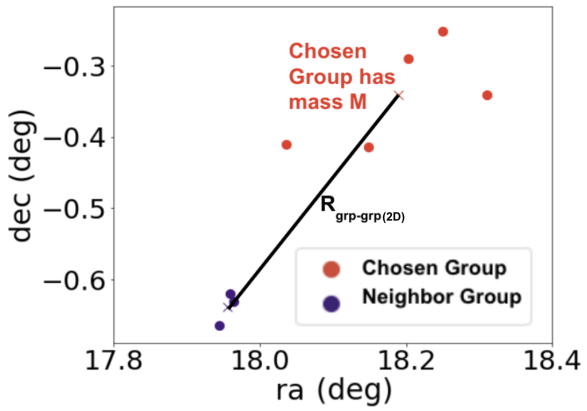

Figure 2: Two nearest neighbor FoF groups, labelled with different colors, with the mass of the chosen group and the projected distance between the group centers needed to calculate the 2D escape velocity labelled.

where $R_{\mathrm{grp-grp\,(3D)}}$ is the 3D distance between the centers of the chosen group and neighbor group and M is the mass of the chosen group (containing N galaxies) given by

$$M = \sum_{N} M_{\mathrm{stellar}} + M_{\mathrm{gas}} + \frac{M_{\mathrm{Halo}}}{N}. \quad (2)$$

An example of two nearest neighbor settled groups with the quantities used for calculating escape velocity labelled is shown in Figure 2. We compare the escape velocity from the nearest neighbor group to the relative velocity between the chosen group and neighbor group, $v_{\mathrm{grp-grp\,(3D)}}$. The chosen group and neighbor group are considered to be bound if $v_{\mathrm{grp-grp\,(3D)}} < v_{\mathrm{escape}}$. If a settled group is found to be bound to its nearest neighbor group, it will be tested for gravitational boundness to its next nearest neighbor settled group until the boundness test finds no more gravitationally-bound neighbor groups. When multiple settled groups are bound to one another, they become classified as a bound multi-group system.

3.1.2. *Projection Effect Corrections*

Observational data can only tell us line-of-sight projected relative velocity between groups, $v_{\mathrm{grp-grp\,(LOS)}} = |cz_{\mathrm{mean,\,chosen\,group}} - cz_{\mathrm{mean,\,neighbor\,group}}|$ and on-sky projected $R_{\mathrm{grp-grp\,(2D)}}$ calculated with the Haversine formula (Gade 2010). Using the on-sky projected $R_{\mathrm{grp-grp\,(2D)}}$ and the line-of-sight projected $v_{\mathrm{grp-grp\,(LOS)}}$ gives rise to projection effects that cause a falsely large number of settled groups to be classified as gravitationally bound to their nearest neighbor group by the boundness method. To correct for these projection effects we use the mock catalogs, which contain three-dimensional true distances and velocities as well as projected distances and velocities that simulate what we would observe. For each pair of nearest neighbor settled groups in the mock catalogs, we calculate both the observed and true $v_{\mathrm{grp-grp}}$ and $R_{\mathrm{grp-grp}}$. We then create distributions of the ratios $v_{\mathrm{grp-grp\,(3D)}}$ / $v_{\mathrm{grp-grp\,(LOS)}}$ and $R_{\mathrm{grp-grp\,(3D)}}$ / $R_{\mathrm{grp-grp\,(2D)}}$ (shown in Figure 3). We have tested these distributions for dependence on halo mass and group multiplicity, and find them to be universal (Figure 4). For each pair of nearby settled groups in RESOLVE and ECO, we multiply the ratio distributions by the calculated $v_{\mathrm{grp-grp\,(LOS)}}$ and $R_{\mathrm{grp-grp\,(2D)}}$ respectively for that pair of neighboring settled groups to obtain distributions of possible $v_{\mathrm{grp-grp\,(3D)}}$ and $R_{\mathrm{grp-grp\,(3D)}}$ values. We use the distribution of $R_{\mathrm{grp-grp\,(3D)}}$ values to calculate a distribution of possible escape velocities using Equation 1. We calculate the probability that the pair is gravitationally bound using Monte Carlo sampling with 10,000 samples each from the v_{esc} and $v_{\mathrm{grp-grp}}$ distributions. We compare each pair of samples, and calculate the probability of boundness as the fraction of all samples where $v_{\mathrm{escape}} > v_{\mathrm{grp-grp}}$. In order for settled groups to be considered part of the same bound multi-group system, the probability that they are bound must exceed 90%. We tested a range of probability thresholds, and chose a 90% threshold because the resulting catalog of bound multi-group systems is most similar to the catalog of bound multi-group systems resulting from 3D boundness testing in the mock catalogs.

3.1.3. *Purity and Completeness of Bound Multi-group Systems*

Figure 5 shows that our method successfully corrects for projection effects in the frequency distribution of group N (multiplicity function) for the mock catalogs. A two-sample Kolmogorov-Smirnov test (Hodges 1958) comparing the multiplicity functions of 3D bound systems and 2D bound systems with projection effect corrections gives a p-value of 0.43, indicating that the two multiplicity functions are very similar and the statistical correction of projection effects is successful. Using the $v_{\mathrm{grp-grp\,(3D)}}$ and $R_{\mathrm{grp-grp\,(3D)}}$ distributions to correct for projection effects enables the statistical correction of the overall number and sizes of bound multi-group systems, which Figure 5 shows is successful, but it does not ensure that each individual group that is tested for boundness will be classified correctly, since some groups' true $v_{\mathrm{grp-grp\,(3D)}}$ and $R_{\mathrm{grp-grp\,(3D)}}$ will be outliers in the distribution of possible values. To study how often individual groups are incorrectly classified using 2D observational data with projection effect corrections, we use the mocks to compare the constituent FoF groups

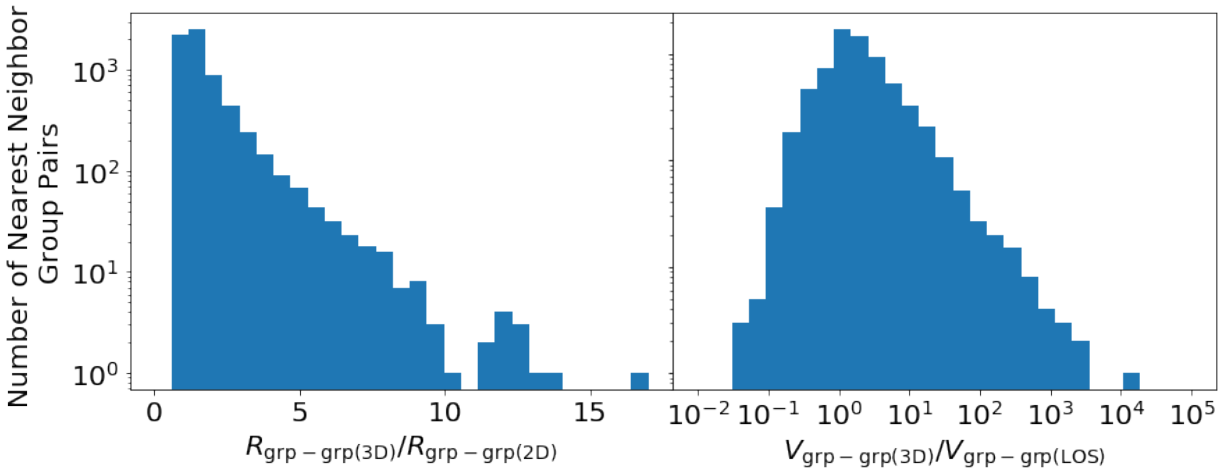

Figure 3: Distributions of $R_{\rm grp-grp\,(3D)}$ / $R_{\rm grp-grp\,(2D)}$ and $v_{\rm grp-grp\,(3D)}$ / $v_{\rm grp-grp\,(LOS)}$ for every pair of nearest neighbor settled groups in the mock catalogs. These distributions are used to statistically correct for projection effects in observational data.

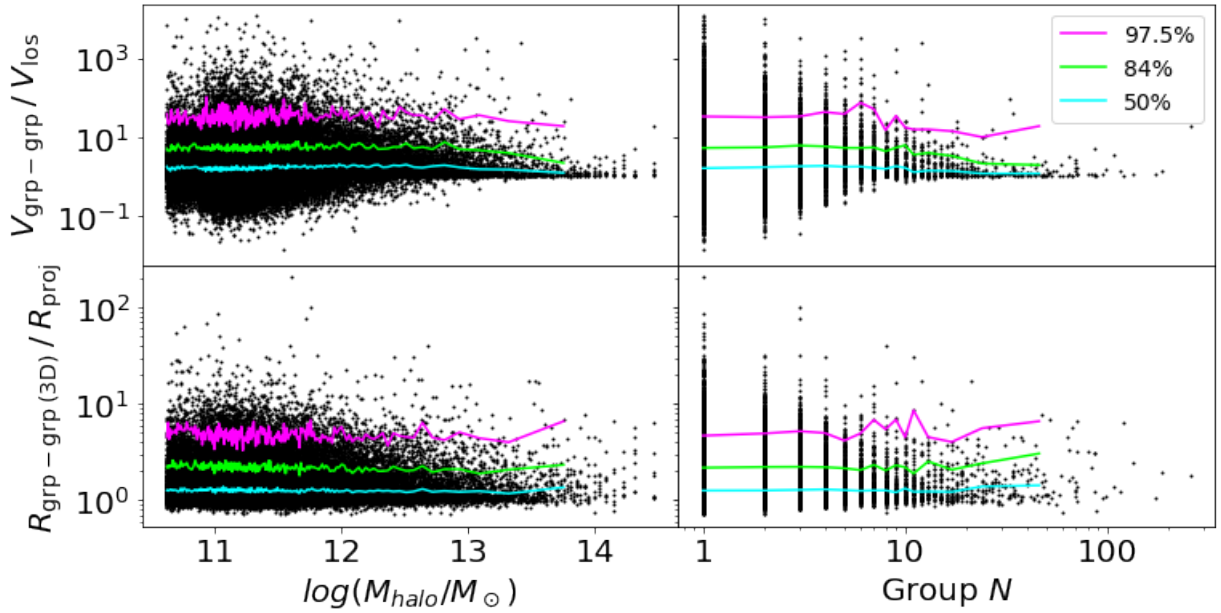

Figure 4: Scatter plots with conditional probabilities of 50%, 84%, and 97.5% over-plotted of ratios $R_{\rm grp-grp\,(3D)}$ / $R_{\rm grp-grp\,(2D)}$ and $v_{\rm grp-grp\,(3D)}$ / $v_{\rm grp-grp\,(LOS)}$ plotted against group halo mass and group multiplicity for FoF groups in the mock catalogs. Since the ratios are constant with respect to group multiplicity and halo mass, we use the entire distribution to correct for projection effects.

contained in each bound multi-group system identified using 2D vs. 3D data. We find that 86% of all bound multi-group systems identified using 2D data contain exactly the same FoF groups as a bound multi-group system identified using 3D data, meaning that the true (3D) bound multi-group system is successfully recovered when observational data with projection effect corrections are used to test for boundness. The remaining 14% of bound multi-group systems identified using 2D data do not match the true (3D) bound multi-group system, and either contain interloper settled groups or are missing settled groups that are truly part of the bound multi-group system. This is an improvement over performing boundness testing using 2D data without projection effect corrections, where 66% of 2D-identified bound multi-group systems are true bound multi-group systems and the remaining 34% contain interlopers or are incomplete. We find high completeness of bound

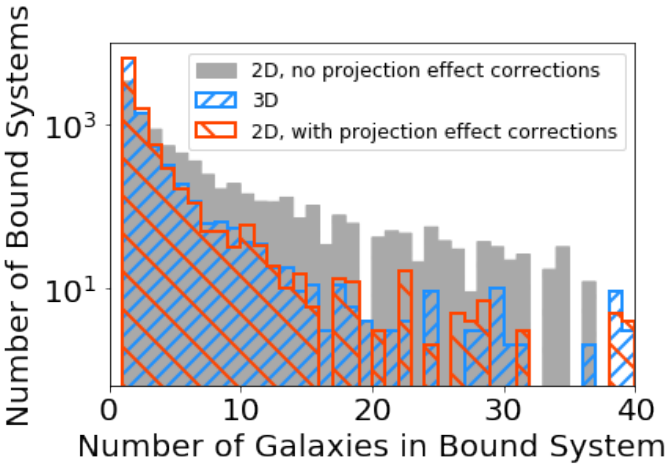

Figure 5: Frequency distributions of group N (multiplicity functions) for bound systems (FoF groups + bound multi-group systems) resulting from boundness testing applied to 3D data and 2D simulated observational data in the mock with and without projection effect corrections. Eleven systems with more than 40 galaxies are excluded in this figure for ease of visual comparison between multiplicity functions. Boundness testing on 3D data is free from projection effects. The similarity of the blue and red histograms (two-sample Kolmogorov-Smirnov test p-value = 0.43) shows that our method is successful in correcting for projection effects in the multiplicity function of bound systems.

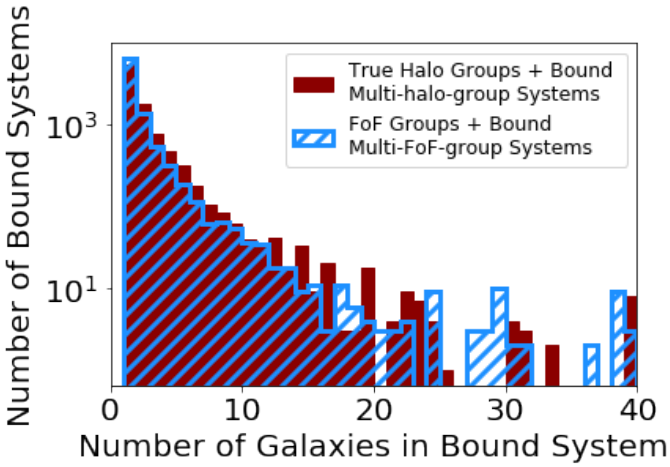

Figure 6: Comparison of the multiplicity functions of bound systems (settled groups + bound multi-group systems) resulting from using the FoF group catalog vs. true halo groups to identify bound multi-group systems using three-dimensional quantities in the mock catalog. A two-sample Kolmogorov-Smirnov test gives a p-value of 0.08. Eleven systems with more than 40 galaxies are excluded for ease of visual comparison between multiplicity functions.

multi-group systems identified with 2D data — 90% of true (3D) bound multi-group systems are also identified using 2D data. Although correcting for projection effects does improve the accuracy of individual groups' classifications as part of bound multi-group systems, about 14% of bound multi-group systems are still classified erroneously due to projection effects, and studying a very small sample of bound multi-group systems could lead to false conclusions even though the overall agreement between the populations of bound systems using 2D projection effect-corrected data and 3D data is very good.

The boundness method relies on a catalog of settled groups as basis for testing for gravitational boundness. Ideally, each settled group consists of all of the galaxies that share a single dark matter halo. However, since it is impossible to directly observe which galaxies share a common halo, we rely on FoF to find settled groups. FoF does an imperfect job of recovering true halo groups (Stothert et al. 2019), and the boundness method inherits these group-finding errors when it tests nearby settled groups for gravitational boundness. We use the mock catalogs, which contain dark matter information that allows us to use true halo groups as the basis for boundness testing, to examine the effects of FoF's group-finding errors on the final catalog of groups and bound multi-group systems. Figure 6 shows a comparison of the multiplicity functions of bound systems (settled groups + bound multi-group systems identified with 3D information) based on a settled group catalog found with FoF and a settled group catalog of the true halo groups in the mock catalogs. A two-sample Kolmogorov-Smirnov test shows that the two distributions are statistically similar, so the group finding errors inherited from FoF do not significantly affect the catalog of bound multi-group systems.

3.1.4. *Bound System Definitions*

We categorize groups and bound multi-group systems based on boundness and halo or system mass. For a bound multi-group system, the system mass is the sum of the halo masses of all of the settled groups in the bound multi-group system. We divide categories of groups and bound multi-group systems by halo or system mass at the bimodality scale of 10^{12} $M_\odot$, the halo mass at which halo gas is heated out to the virial radius, shutting off cold flows of gas that would fuel star formation (Dekel & Birnboim 2006).

With the understanding that a settled group is a FoF group consisting of a single galaxy or multiple galaxies,

we use the following definitions to classify our settled groups and bound multi-group systems.

- Small settled group: a settled group of one or more galaxies with a halo mass of less than 10^{12} $M_{\odot}$.
- Large settled group: a settled group of one or more galaxies with a halo mass of greater than 10^{12} $M_{\odot}$. An example of a large settled group is shown in panel (a) of Figure 7.
- Proto-group (small bound multi-group system): a bound multi-group system with a total system mass of less than 10^{12} $M_{\odot}$. An example of a proto-group is shown in panel (b) of Figure 7.
- Large bound multi-group system: a bound multi-group system with a total system mass of greater than 10^{12} $M_{\odot}$. An example of a large bound multi-group system is shown in panel (c) of Figure 7.

3.2. *Local Group Analogues*

3.2.1. *Selection Criteria for Local Group Analogues*

We identify Local Group analogues as a subset of bound multi-group systems, based on criteria used to find LG analogues in previous papers outlined in Table 1. All of the papers listed in Table 1 identified LG analogues in simulations. Each of our LG analogues contains two giant galaxies: a MW analogue and an M31 analogue, and the satellites associated with the giant galaxies by FoF. We tested several different combinations of selection criteria for LG analogues from Table 1, and settled on using the mass and separation constraints used by Carlesi et al. (2019) so that the samples of LG analogues in RESOLVE and ECO would be large enough for statistical comparisons. Following Carlesi et al. (2019), we impose a set of three mass constraints: the MW and M31 analogues must each have a halo mass of greater than 5×10^{11} $M_{\odot}$/h, their combined halo mass must be less than 5×10^{12} $M_{\odot}$/h, and the halo mass of the M31 analogue must be no more than three times greater than the halo mass of the MW analogue. We also use the separation constraint from Carlesi et al. (2019) that the MW and M31 analogues must be separated by between 0.35 and 1.25 Mpc/h. When identifying Local Group analogues using observational data, we use the distribution of $R_{\mathrm{grp-grp\,(3D)}}$ / $R_{\mathrm{grp-grp\,(2D)}}$ obtained from the mock catalogs to correct for projection effects in the distance calculation. We multiply the projected distance between the MW and M31 analogues by the $R_{\mathrm{grp-grp\,(3D)}}$ / $R_{\mathrm{grp-grp\,(2D)}}$ distribution to obtain a distribution of possible 3D separations, and require that the median of that distribution be between 0.35 and 1.25 Mpc/h. We use $h = 0.7$.

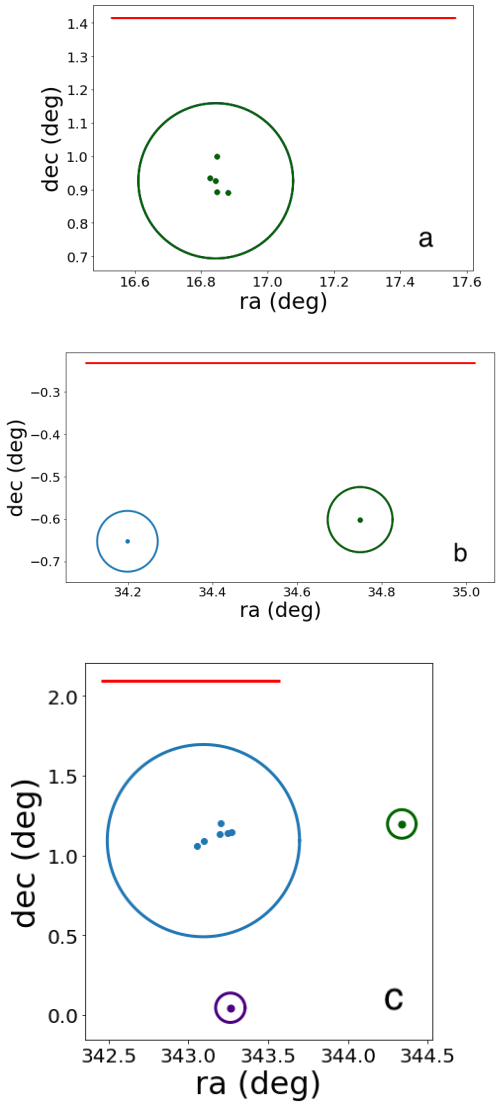

Figure 7: Plots showing how (a) a large settled group, (b) a proto-group, and (c) a large bound multi-group system in RESOLVE appear projected on the sky. The points represent galaxies and are color coded by the FoF group that they belong to. The circles show the virial radius of each FoF group, which represents the extent of the group's dark matter halo (see Equation 3). Red line at top of sky plot is scale bar showing 1 Mpc projected onto the sky.

To ensure that the Local Group analogue is isolated and physically associated, we use the boundness method instead of the isolation and velocity constraints used in previous work. We require that the MW and M31 analogue halos be gravitationally bound to each other, and that neither are gravitationally bound to a third mas-

sive group with halo mass greater than $10^{11.5} M_{\odot}$, the gas-richness threshold halo mass that we define as the dwarf-giant divide (Kannappan et al. 2013; Eckert et al. 2016). By requiring that the two halos in the Local Group analogue are bound to each other and that neither are bound to any third giant halo, we ensure that the Local Group analogue is gravitationally bound and evolving without the influence of other large groups or clusters, accomplishing the same goal as the velocity and isolation constraints used in previous work.

3.2.2. *Purity and Completeness of Local Group Analogues*

We identify two separate populations of LG analogues in the mock catalogs: a "true" population using three-dimensional data and an "observational" population identified using projection effect-corrected simulated observational data. We compare these two populations to gain an understanding of how severely projection effects distort the true population of LG analogues. Projection effects factor into three steps in our identification of LG analogues: the calculation of the distance between the MW and M31 analogues to determine if the pair meets the separation criterion, the determination of whether the MW and M31 analogues are gravitationally bound to one another, and the determination of whether the MW or M31 analogues are bound to any other massive galaxies to test whether the pair meets the isolation criterion. To assess both the completeness and purity of the simulated observational LG analogues relative to the true LG analogues, we have tested whether each true LG analogue was also identified as a LG analogue using observational quantities and vice versa. We find high completeness: 89% of all true LG analogues are also identified as observational LG analogues. However, we find lower purity: within the population of observational LG analogues, the percentage of true LG analogues is 73%, and the remaining 27% of observational LG analogues are spurious.

3.2.3. *The Boundness Method Applied to Local Group Analogues*

To ascertain how well the boundness method finds groups like the Local Group when applied to real data, we tested whether each true Local Group analogue identified using 3D data in the mock catalogs is classified as a bound multi-group system by the boundness method. Using the simulated observational data available in the mock catalogs, we find that 97% of all true Local Group analogues based on 3D data are classified as bound multi-group systems by the boundness method using projection effect-corrected simulated observational quantities. FoF, which identifies settled groups in the mock catalogs using observational quantities, identifies ∼6% of all true Local Group analogues in the mock catalogs as a settled group. Since the FoF linking lengths used in the mock catalogs are calibrated to optimally recover groups that share a common dark matter halo, it is not surprising that few FoF groups qualify as Local Group analogues. Our findings in the mock catalogs confirm that the boundness method succeeds in finding groups like our own Local Group that are in early formation stages.

4. RESULTS

4.1. *Overview of Bound Multi-group Systems in RESOLVE and ECO*

Comparisons between the catalog of settled groups before boundness testing and the catalog of bound systems after boundness testing help us understand how common bound multi-group systems are, and how their properties differ from those of settled groups. The frequency of each type of group or system, and the percentage of galaxies that belong to each type of group or system before and after boundness testing in a combined sample of RESOLVE-B and ECO is shown in Figure 8. When boundness testing is performed, the number of $N = 1$ groups decreases, illustrating that many galaxies that reside in their own halos are gravitationally bound in proto-groups or large bound multi-group systems. After boundness testing in ECO, 21% of galaxies are members of a bound multi-group system, 30% of galaxies are members of a multiple-member settled group, and 49% of galaxies is an $N = 1$ group. A summary of the number and frequency of each type of bound system in RESOLVE and ECO after boundness testing is shown in Table 2.

Figure 9 shows comparisons of the multiplicity function (panel a) and system mass function (panel b) before and after boundness testing in RESOLVE and in ECO (with the RESOLVE-A sub-volume removed). The multiplicity functions show a decrease in the number of $N = 1$ groups and an increase in the number of multiple-galaxy systems of every size when boundness testing is performed. The system mass functions of groups and systems show a similar result; the number of low-mass systems (group or system mass below $\sim 10^{11.5} M_{\odot}$) decreases and the number of high-mass systems increases after boundness testing.

4.2. *Does the Boundness Method Find Groups in Early Formation Stages?*

Comparisons of group and system properties and environments are necessary to test whether the boundness method succeeds in identifying systems that could evolve into settled groups. Below we test how com-

	Mass Constraint	Separation Constraint	Isolation Constraint	Relative Velocity Constraint
Li and White 2007	No constraint	0.5 - 1 Mpc	• No cluster with $M_{vir} > 3 \times 10^{13} M_{\odot}$ within 3 Mpc • No galaxy with max. rotational velocity >150 km/s within 1 Mpc	Negative relative radial velocity
Carlesi et al 2019	• Halo mass of each giant galaxy $> 0.5 \times 10^{12} M_{\odot}/h$ • Total halo mass of pair $< 5 \times 10^{12} M_{\odot}/h$ • Halo mass ratio $M_{M31}/M_{MW} < 3$	0.35 - 1.25 Mpc/h	No third halo of mass $> M_{MW}$ located within 2.5 Mpc/h	Negative relative radial velocity
Meng Zhai et al 2020	• Stellar mass 4×10^{10} - 8×10^{10} $M_{\odot}$for MW analogue • Stellar mass 8×10^{10} - 1.3×10^{11} $M_{\odot}$for M31 analogue	0.6 - 1 Mpc	No third halo of mass $> M_{MW}$ located within 2.5 Mpc	Negative radial velocity between -190 and -135 km/s
Fattahi et al 2015	Total halo mass of pair in the range 1.6×10^{12} - 3.4×10^{12} $M_{\odot}$	0.6 - 1 Mpc	No constraint	Negative radial velocity between -250 and 0 km/s
Garrison-Kimmel et al 2018	Halo mass of each giant galaxy 1×10^{12} - 2×10^{12} $M_{\odot}$	0.84 -0.92 Mpc	No constraint	Negative radial velocity between -107 and -93 km/s

Table 1: Criteria used to define Local Group analogues in simulations in previous work.

	RESOLVE # (%) of bound systems	ECO # (%) of bound systems	RESOLVE # (%) of galaxies	ECO # (%) of galaxies
Singles	694 (75%)	6270 (77%)	694 (48%)	6270 (49%)
N>1 Small Settled Groups	91 (11%)	842 (10%)	208 (14%)	1900 (15%)
N>1 Large Settled Groups	49 (5%)	427 (5%)	176 (12%)	1863 (15%)
Proto-groups	40 (4%)	311 (4%)	101 (7%)	787 (6%)
Large Bound Multi-group Systems	930 (5%)	303 (4%)	256 (18%)	1878 (15%)

Table 2: Table showing how common each type of bound system is in RESOLVE and ECO after boundness testing. The number of each type of system, the percentage of each type of system among all systems, the number of galaxies that are members of each type of system, and the percentage of all galaxies that are members of each type of system in both RESOLVE and ECO are shown.

monly the virial radii of settled groups within bound multi-group systems overlap, use the Anderson-Darling test and group crossing time to compare the virialization states of bound multi-group systems and settled groups, and compare the local environments in which proto-groups and small settled groups reside.

4.2.1. *Halo Overlap in Bound Multi-group Systems*

To get a sense of whether our bound multi-group systems are already physically interacting systems, we calculate whether the virial radii of the constituent settled groups that make up bound multi-group systems are overlapping, similar to the Tempel et al. (2017) test for merging groups. A group's virial radius is an approximation of the extent of the group's dark matter halo, and is calculated from the halo mass of the group with

$$R_{vir} = \left(\frac{3 M_h}{4\pi \Delta_{mean} \Omega_m \rho_c} \right)^{1/3}, \quad (3)$$

where M_h is the halo mass of the settled group (before calculating the virial radius we convert all halo masses to M337b, the mass contained within a region 337 times the background density of the Universe, from

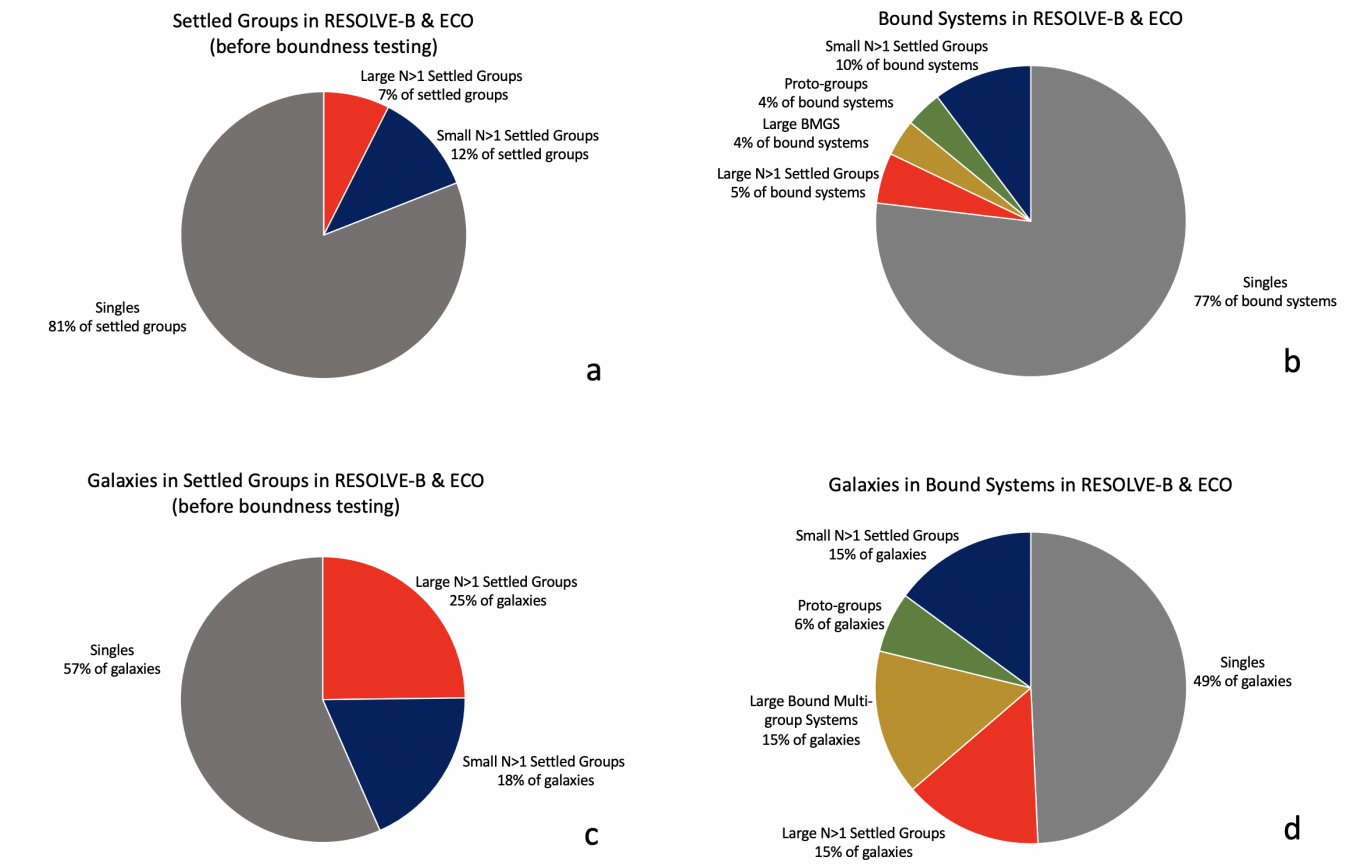

Figure 8: Pie charts showing (a) the frequency of each type of settled group among all settled groups before boundness testing, (b) the frequency of each type of bound system among all bound systems after boundness testing, (c) the percent of all galaxies that belong to each type of settled group before boundness testing, and (d) the percent of all galaxies that belong to each type of bound system after boundness testing in a combined sample of ECO and RESOLVE-B.

M280b in RESOLVE and ECO and M200b in the mock catalogs using the method of Hu & Kravtsov 2003), Δ_{mean} is the overdensity threshold above the mean background density of the Universe that is used to define a group's dark matter halo (for virial radius calculations, we use $\Delta_{mean} = 337$ following Bryan & Norman 1998), $\Omega_m = 0.3$ is the matter density of the Universe, and $\rho_c = 2.77 \times 10^{11}\ h^2\ M_\odot/\mathrm{Mpc}^3$ is the critical density of the Universe. We calculate whether the virial radii of two nearby FoF groups in RESOLVE or ECO are overlapping by comparing the sum of the two groups' virial radii to the distance between the group centers (the projected distance that has been corrected for projection effects using the median of the distribution of $R_{\mathrm{grp-grp\ (3D)}}$ / $R_{\mathrm{grp-grp\ (2D)}}$ values). We do not test for overlap along the line-of-sight direction. If the distance between the group centers is smaller than the groups' combined virial radii, then we conclude that the virial radii of the two groups are overlapping, and their halos may be interacting. The percentage of bound multi-group systems containing FoF groups with overlapping virial radii is 18% of all bound multi-group systems in RESOLVE and 22% in ECO. Figure 10 shows two examples of bound multi-group systems in RESOLVE that contain overlapping virial radii. We also test for on-sky halo overlap in the mock catalogs, where we find that the percentage of bound multi-group systems containing FoF groups with overlapping virial radii is 21%, closely agreeing with the observational values from RESOLVE and ECO.

4.2.2. *Anderson-Darling Test for Bound Multi-group Systems and Settled Groups*

We use the Anderson-Darling test to quantify the virialization state of settled groups and bound multi-group systems. The Anderson-Darling test assesses the normality of a group's velocity distribution. The closer to normal a group's velocity distribution is, the more virialized, or settled into equilibrium, the group is. We

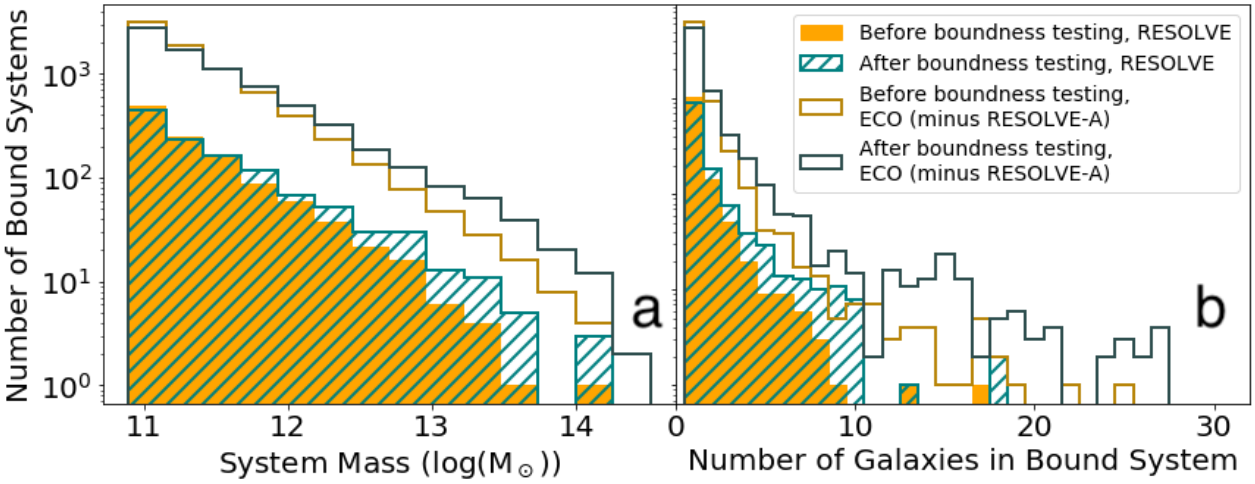

Figure 9: RESOLVE and ECO (minus RESOLVE-A) multiplicity and system mass functions before boundness testing (FoF groups) and after boundness testing (FoF groups including $N = 1$ groups + bound multi-group systems). (a) System mass function of groups (HAM halo mass) and bound systems (sum of HAM halo masses) before and after boundness testing. (b) Multiplicity function of groups and bound systems before and after boundness testing. One bound multi-group system in RESOLVE and 14 in ECO with more than 30 galaxies are excluded for ease of visual comparison.

follow the method described by Hou et al. (2009) for conducting the Anderson-Darling test and calculating an α value for each group that represents the probability that the group's velocity distribution follows a normal distribution (although α values can exceed 1). The Anderson-Darling test can be done for groups with more than 5 member galaxies. The results of the Anderson-Darling test for every $N > 5$ settled group and bound multi-group system in ECO and RESOLVE-B is shown in Figure 11.

The distribution of α values for bound multi-group systems has smaller peak and median α values than the distribution for settled groups. This result suggests that bound multi-group systems are less virialized than settled groups at 2.5σ confidence, which aligns with what we would expect for groups in the early stages of formation. It is interesting to note that while bound multi-group systems are on average less virialized than settled groups, most still fall above the threshold for being virialized set by Hou et al. (2009) of $\alpha = 0.05$. This suggests that bound multi-group systems, although not as settled into equilibrium as settled groups, have still reached a partially virialized stage of evolution.

4.2.3. *Group Crossing Time of Proto-groups and Small Settled Groups*

The Anderson-Darling test is one way of measuring the virialization state of groups, but the test can only be performed for groups with $N > 5$ members and so is not ideal for studying small groups like proto-groups and small settled groups. For these smaller systems we use group crossing time instead. The crossing time of a group is the time it would take a member galaxy to cross the length of the group. Groups with smaller crossing times are more virialized than groups with longer crossing times. To calculate the crossing times of proto-groups and small settled groups, we follow the method used in Firth et al. (2006):

$$t_c = \frac{\langle r \rangle}{\langle |v| \rangle}, \tag{4}$$

where $\langle r \rangle$ is the average projected distance of group members from the group's center of mass and $\langle |v| \rangle$ is the average speed of group members relative to the group center of mass.

Figure 12 compares the distributions of crossing times for proto-groups and small settled groups, showing that proto-groups have overall higher crossing times, which is as we would expect since higher crossing times indicate that groups are less virialized. The median crossing time for proto-groups is about 100 times longer than the median crossing time for small settled groups (108 Gyr for proto-groups vs. 1.2 Gyr for small settled groups). Although many proto-groups appear far from virialization, with crossing times much greater than the age of the Universe, there is some overlap between the distributions for the two types of groups because the crossing times vary over many orders of magnitude. Proto-groups and small settled groups contain a wide range of different virialization states. We find that 21% of proto-groups and 95% of small settled groups have crossing times less than the age of the Universe. Of the proto-

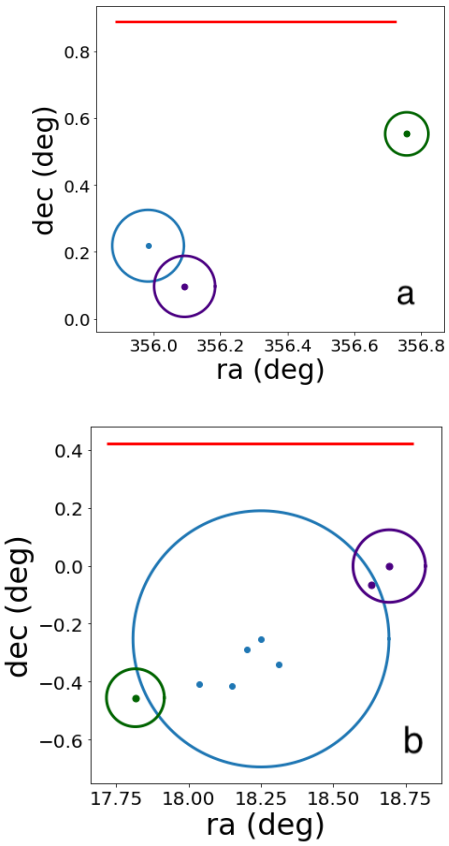

Figure 10: Plots showing the projected positions of galaxies in bound multi-group systems and the virial radii of the constituent FoF groups. (a) A proto-group containing overlapping virial radii, (b) A large bound multi-group system with virial radii overlapping, suggesting interacting dark matter halos. Both groups are in the RESOLVE survey. Red line at top of sky plot is scale bar showing 1 Mpc projected onto the sky.

groups with crossing time less than the age of the Universe, 55% also contain overlapping dark matter halos according to the method from Section 4.2.1, so these proto-groups seem to be furthest along in their evolution and closest to merging. We use the true halo group membership information available in the mock catalogs as well as the FoF group membership to determine how many of the small settled groups with crossing time longer than the age of the Universe are true halo groups and how many are the result of group finding errors. We find that 36% of settled groups with crossing time larger than the age of the Universe in the mock catalogs are the result of group finding errors where FoF falsely joins together two halo groups. This result from the mock catalogs suggests that some of the small settled groups in RESOLVE and ECO with very large crossing times could actually contain multiple dark matter halos.

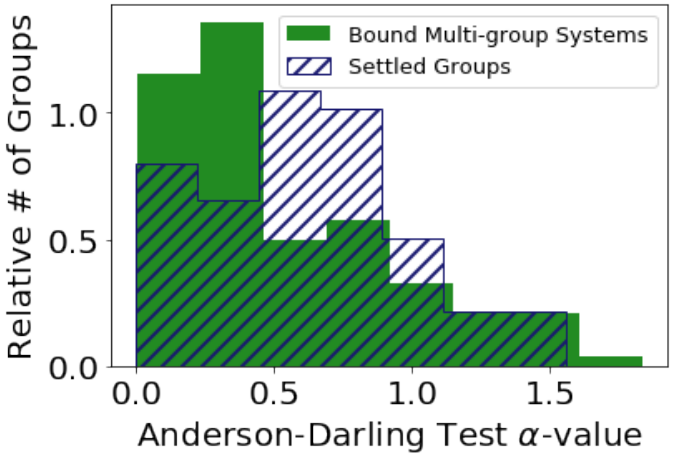

Figure 11: Comparison of Anderson-Darling test α values for settled groups vs. bound multi-group systems with more than 5 member galaxies in ECO and RESOLVE-B. The median α value for bound multi-group systems is 0.42±0.04, while the median α value for settled groups is 0.60±0.05 (uncertainties determined by smoothed bootstrapping as in Wang 1995). The p-value from a two-sample Kolmogorov-Smirnov Test is 0.013. From this p-value, we conclude that the distributions may be different at 2.5σ confidence.

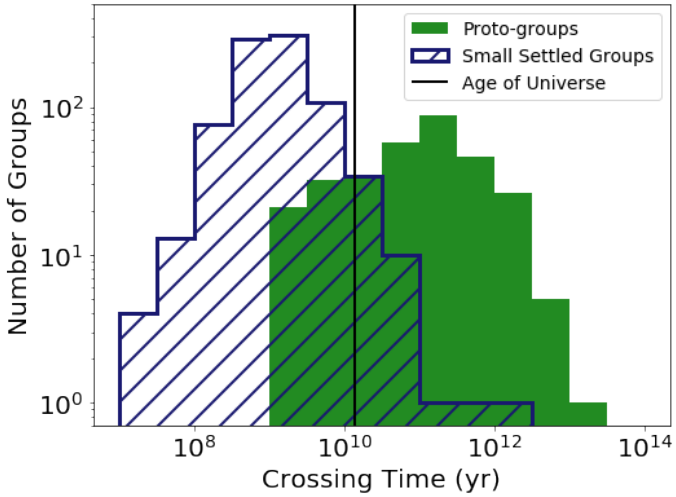

Figure 12: Group crossing time for proto-groups and small settled groups in ECO and RESOLVE-B, calculated using Equation 4. The p-value from a two-sample Kolmogorov-Smirnov test is 1.6×10^{-12}, reflecting the much longer crossing times of proto-groups compared to small settled groups.

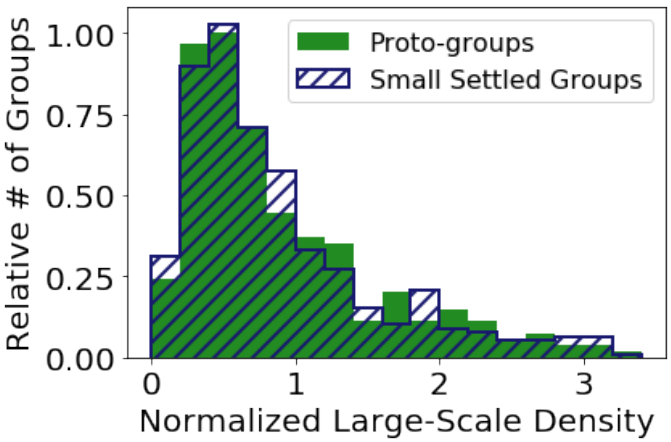

Figure 13: Comparison of the normalized large-scale environmental density around proto-groups vs. small settled groups in ECO. A two-sample Kolmogorov-Smirnov Test gives a p-value of 0.69, indicating that proto-groups and small settled groups reside in the same environments.

4.2.4. *Environmental Comparison of Proto-groups and Small Settled Groups*

To assess whether proto-groups could be groups in the early stages of formation that will eventually evolve into small settled groups, we compare the environments in which the two types of groups are found in ECO. Figure 13 shows a comparison of the normalized large-scale environmental density between proto-groups and small settled groups. We use the large-scale environmental density metric that was applied to ECO in Stark et al. (2016) following the method from Carollo et al. (2013). The environmental density is calculated for a group using the halo mass and area enclosed within a circle with a radius of the projected distance from the group to its third nearest neighbor group. The environmental density is normalized to the median density of groups in ECO. The distributions of environmental density for proto-groups and small settled groups are statistically the same according to a two-sample Kolmogorov-Smirnov test, meaning that proto-groups and small settled groups exist in the same large-scale environments. This could make an evolutionary connection between the two types of groups possible.

4.3. *Quantifying the Evolutionary State of Proto-groups and Small Settled Groups*

4.3.1. *Gas Content Comparison*

We look at the how the system integrated gas-to-stellar mass ratios of proto-groups and small settled groups change with system mass to assess whether merging into a single common halo affects the evolution of overall gas content. Figure 14 shows a decrease in the gas content of small settled groups and proto-groups up to the $10^{12} M_{\odot}$ limit built into our definition of these systems (Section 3.1). Shock heating of halo gas is expected starting in halos above the gas-richness threshold halo mass of $10^{11.5} M_{\odot}$ (Kannappan et al. 2013). The decrease in the gas content of small settled groups, which share a common dark matter halo, across the threshold scale in Figure 14 is consistent with this expectation. Although proto-groups do not share a single common halo, 77% of proto-groups in ECO and RESOLVE-B with system mass above the threshold mass scale contain at least one FoF group that is itself above the threshold mass scale, and so would experience halo gas heating, which may explain why the gas content of proto-groups decreases over the threshold mass scale. Two-sample Kolmogorov-Smirnov tests comparing the distributions of gas content of proto-groups and small settled groups in each mass bin show no statistical difference between the two distributions at any system mass. To test whether the gas content of proto-groups may be systematically higher than small settled groups we performed a linear fit to the gas content versus system mass relation for the combined sample of proto-groups and small settled groups. We used the slope from the fit to calculate the y-intercept for proto-groups and small settled groups separately. We found that the y-intercepts for proto-groups and small settled groups differed by less than their uncertainties, and concluded that there is no significant vertical offset between the two distributions.

Since Figure 12 demonstrates that the crossing times of proto-groups and small settled groups differ very significantly, we also test whether the gas content of proto-groups differ from small settled groups as a function of crossing time, shown in Figure 15. The crossing times of proto-groups and small settled groups overlap in three crossing time bins. Two-sample Kolmogorov-Smirnov tests show that the gas contents of small settled groups are higher than the gas contents of proto-groups at 2.2σ, 3σ, and 2.5σ confidence in the three crossing time bins containing both proto-groups and small settled groups. This result suggests that as proto-groups virialize and settle into a common halo the gas content of the group may increase.

Figure 16 shows a bivariate analysis of system mass versus crossing time with contours showing groups gas content in two-dimensional bins for proto-groups and small settled groups. The analysis for small settled groups shows that the small settled groups with the highest gas content mostly have low halo mass and low crossing times. The small settled groups with the lowest gas content also have low crossing times, but have high

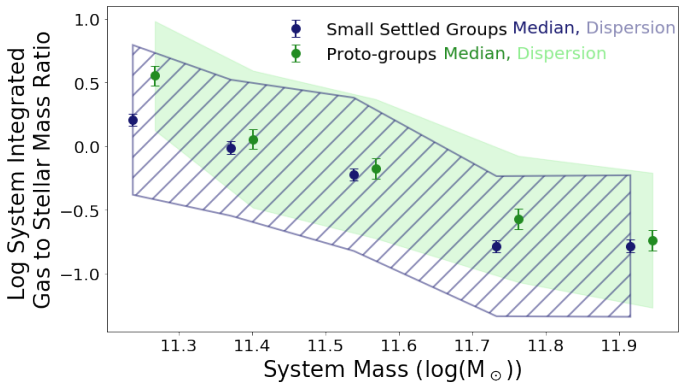

Figure 14: System integrated gas-to-stellar mass ratio vs. system mass for proto-groups and small settled groups in ECO and RESOLVE-B. In each system mass bin we plot the median and uncertainty in the median (as determined by smoothed bootstrapping). We also show the natural $\pm 1\sigma$ spread in group gas content as shaded/hatched regions. The bin center system masses of small settled groups are offset 0.03 dex towards lower system mass to allow for easier visual comparison with proto-groups.

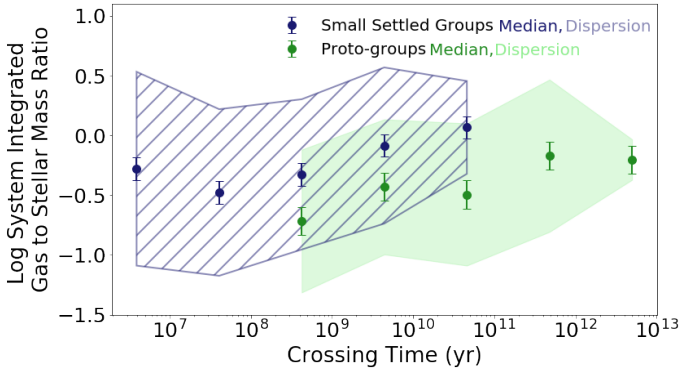

Figure 15: System integrated gas-to-stellar mass ratio vs. crossing time for proto-groups and small settled groups in ECO and RESOLVE-B. In each crossing time bin we plot the median and uncertainty in the median (as determined by smoothed bootstrapping). We also show the natural $\pm 1\sigma$ spread in group gas content as shaded/hatched regions.

halo mass. Proto-groups with high gas content are concentrated at low system mass, while proto-groups with low gas content are concentrated at high system mass.

4.3.2. *Color Gap Comparison*

The u-r "color gap" of a group or system is the difference in u-r color between the central (brightest galaxy in the group in the r-band) and the brightest satellite (Eckert et al. 2017). The color gap of a group or system reflects the degree of quenching that the system has experienced. Since halo gas heating begins at the center of a halo at the gas-richness threshold halo mass scale, the central galaxy in a group is expected to quench before the satellites. A large color gap indicates that the central galaxy has quenched while the satellite has not yet. A small color gap can either indicate that none or all of the galaxies in a group have quenched. Figure 17 shows a comparison of color gap in proto-groups and small settled groups binned by system mass. Since proto-groups and small settled groups by definition have system masses below the bimodality scale and thus their halo gas is not predicted to have heated out to the virial radius yet, we do not expect them to be fully quenched. We see an increase in color gap in small settled groups across the threshold mass scale as the central galaxy in the group begins to quench. Proto-groups do not show a clear trend in color gap with system mass, although two-sample Kolmogorov-Smirnov tests comparing the distributions of color gap for proto-groups and small settled groups do not show a statistically significant difference above 2σ confidence between the distributions in any system mass bin.

We compare the u-r color gap of proto-groups and small settled groups as a function of crossing time in Figure 18. We find that in the crossing time bins containing both proto-groups and small settled groups, two-sample Kolmogorov-Smirnov tests show no difference between the distributions of color gap for proto-groups and small settled groups above 2σ significance. We conclude that the color gaps of proto-groups and small settled groups are similar as a function of both system mass and crossing time, suggesting that the act of settling into a common halo does not significantly affect the progress of quenching in small groups.

4.4. *Local Group Analogues*

We identify Local Group analogues in RESOLVE and ECO using the criteria described in Section 3. In RESOLVE and ECO, LG analogues make up about 13% of all multiple-member galaxy systems, and about 8% of all galaxies are members of a LG analogue. LG analogues are a mix of high-mass proto-groups and low-mass large bound multi-group systems, as shown in Table 3. The combined halo masses of the MW and M31 analogues vary between $\log(M_h/M_\odot) = 11.8 - 12.5$. Each LG analogue consists of the giant MW and M31 analogues, as well as any satellites in their FoF groups. Examples of how some LG analogues in RESOLVE appear on the sky are shown in Figure 19.

Crossing Time:

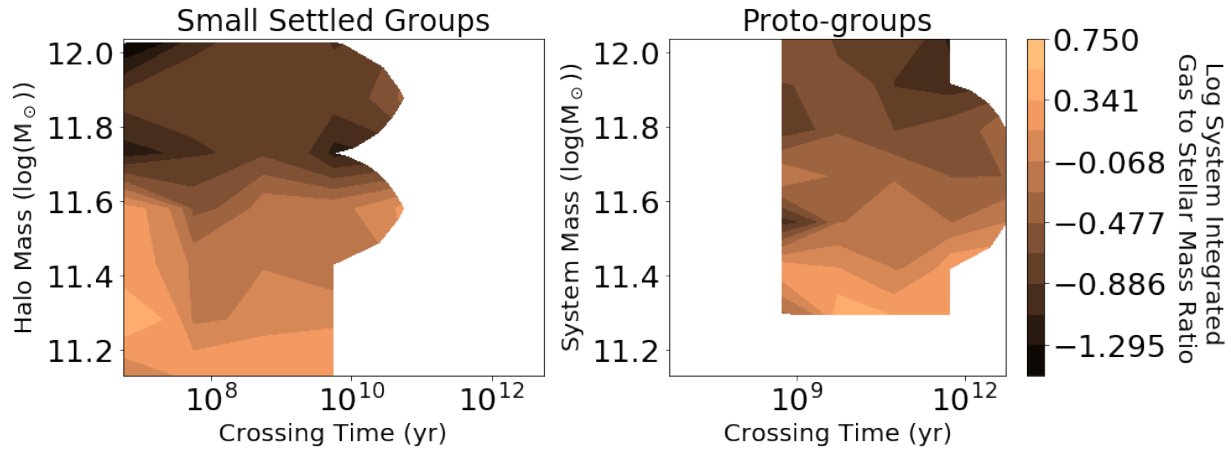

Figure 16: System mass vs. crossing time with contours showing group integrated gas-to-stellar mass ratio for proto-groups and small settled groups.

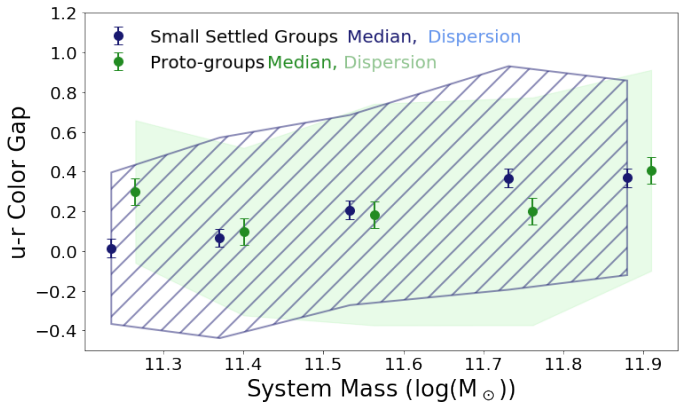

Figure 17: Color gap vs. system mass for proto-groups and small settled groups in ECO and RESOLVE-B. In each system mass bin we plot the median and uncertainty in the median (as determined by smoothed bootstrapping). We also show the natural $\pm 1\sigma$ spread in color gap as shaded/hatched regions. The bin center system masses of small settled groups are offset 0.03 dex towards lower system mass to allow for easier visual comparison with proto-groups.

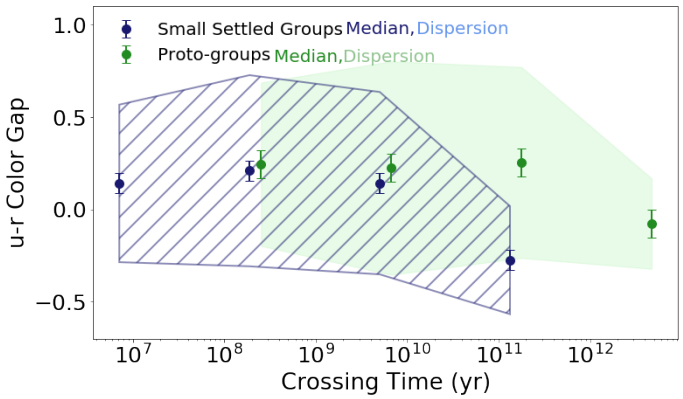

Figure 18: Color gap vs. crossing time for proto-groups and small settled groups in ECO and RESOLVE-B. In each crossing time bin we plot the median and uncertainty in the median (as determined by smoothed bootstrapping). We also show the natural $\pm 1\sigma$ spread in color gap as shaded/hatched regions. The bin center crossing times of small settled groups are offset slightly towards lower crossing time to allow for easier visual comparison with proto-groups.

	RESOLVE	ECO
Number of LG Analogues	32	229
% of LG Analogues that are Proto-groups	16%	84%
% of LG Analogues that are Large Bound Multi-Group Systems	26%	74%

Table 3: Overview statistics for LG analogues in RESOLVE and ECO.

We compare group crossing times of Local Group analogues to the crossing times of a control sample of non-LG-analogue bound multi-group systems with matched total system mass $10^{11.8} - 10^{12.5} M_{\odot}$ to assess relative virialization state. Figure 20 shows that the crossing times of LG analogues are more concentrated at low crossing time (thus, more virialized) than the control sample. The median crossing time for LG analogues is about 3 times shorter (4.2 Gyr for LG analogues vs. 13 Gyr for the control sample). 84% of LG analogues have crossing times less than the age of the Universe. For reference in comparing timescales, we note that Cox & Loeb (2008) estimate with simulations that the Milky

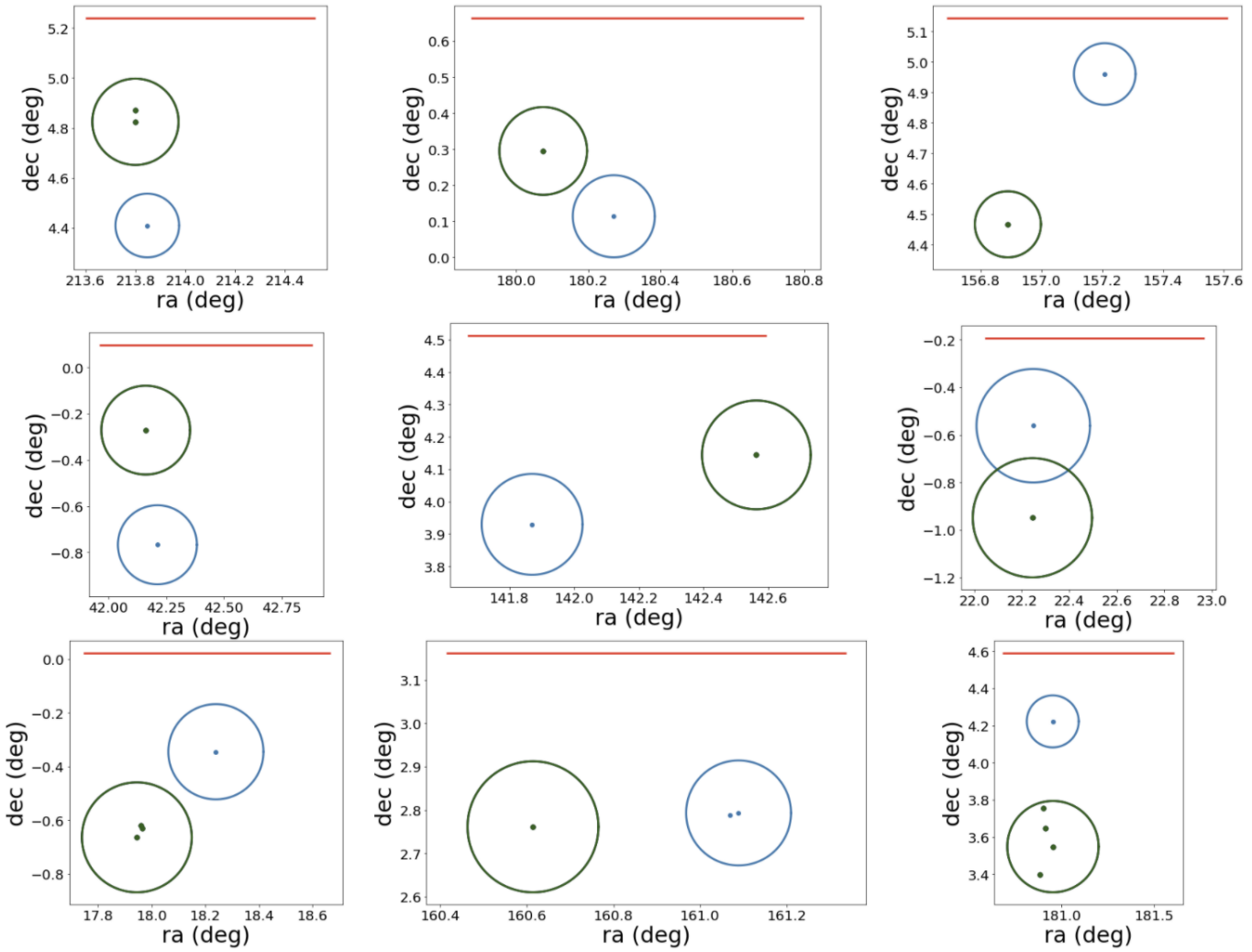

Figure 19: Nine on-sky projected examples of Local Group analogues in RESOLVE. The MW analogue is shown in blue and the M31 analogue is shown in green. The points represent the locations of the galaxies and the circles represent the extent of the virial radii of the FoF groups. The red scale bar shows 1 Mpc projected onto the sky.

Way and Andromeda will make their first close passage in 2.8 Gyr and merge in 5.4 Gyr, so the crossing times of 1-10 Gyr we find for most LG analogues are consistent with predictions for the real Local Group.

Environments:

We compare the large-scale environment around LG analogues to the large-scale environment around non-LG-analogue bound multi-group systems with matched total system mass in Figure 21. LG analogues are more commonly found in less dense environments than other bound multi-group systems of similar mass. This result may reflect the isolation criteria that we use to identify LG analogues.

Halo Overlap:

Following the method described in Section 4.2.1, we calculate the fraction of all Local Group analogues in which the virial radii of the MW and M31 analogue FoF groups overlap, and we compare to the fraction of mass-matched non-LG analogue bound multi-group systems containing FoF groups whose virial radii overlap. We find that in RESOLVE-B and ECO, 14% of LG analogues contain overlapping virial radii, and 13% of bound multi-group systems in the control sample contain overlapping virial radii. The frequencies of overlapping virial radii in the LG analogue and mass-matched control samples are smaller than the frequency in all bound multi-group systems of 18% in RESOLVE and 22% in ECO from Section 4.2.1. This difference is because bound multi-group systems with system masses higher than the range allowed for LG analogues contain FoF groups with larger virial radii, and are more likely to contain overlapping halos.

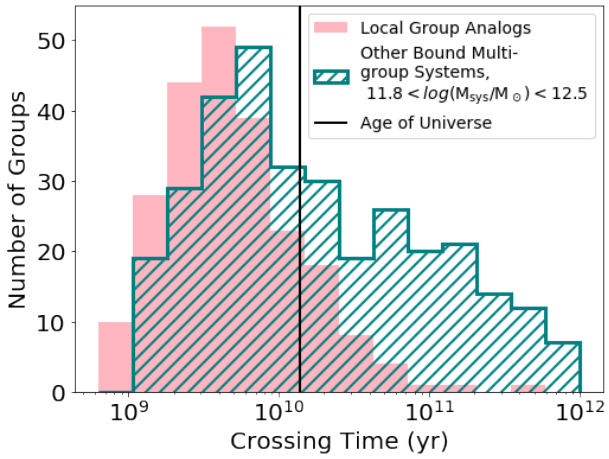

Figure 20: Group crossing times for Local Group analogues and for a mass-matched control sample of non-LG-analogue bound multi-group systems in ECO and RESOLVE-B. Smaller group crossing times are indicative of more virialized groups. The p-value from a two-sample Kolmogorov-Smirnov test is 3.3×10^{-15}, showing that LG analogues are more virialized at very high confidence.

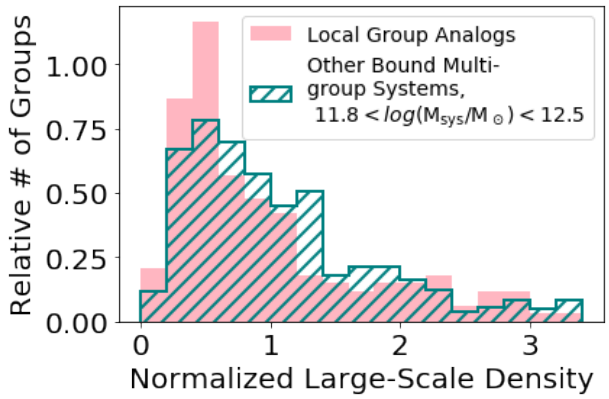

Figure 21: Large-scale environment (as in section 4.2.4) around Local Group analogues and around non-LG analogue bound multi-group systems with similar system mass in ECO. The p-value from a two-sample Kolmogorov-Smirnov test is 3×10^{-3}, indicating that LG analogues occupy less dense environments at 3σ confidence.

Gas Content:

We compare the system integrated gas-to-stellar mass ratio of LG analogues and the mass-matched control sample over the range of system mass spanned by LG analogues. Figure 22 shows that for both LG analogues and the control sample, gas content decreases with system mass. Two-sample Kolmogorov-Smirnov tests comparing the distributions of gas-to-stellar mass ratio for

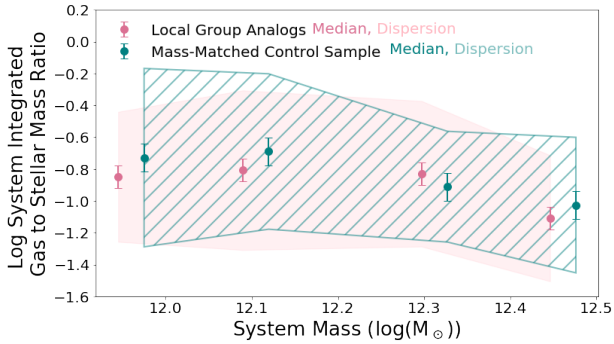

Figure 22: System integrated gas-to-stellar mass ratio vs. system mass for LG analogues and the mass-matched control sample of non-LG analogue bound multi-group systems in ECO and RESOLVE-B. In each system mass bin we plot the median and uncertainty in the median (as determined by smoothed bootstrapping). We also show the natural $\pm 1\sigma$ spread in group gas content as shaded/hatched regions. The bin center system masses of LG analogues are offset 0.03 dex towards lower system mass to allow for easier visual comparison with the control sample.

LG analogues and the control sample in each system mass bin show no statistical differences between the distributions.

Figure 23 shows gas content vs. crossing time for LG analogues and bound multi-group systems in the mass-matched control sample. In the crossing time bins containing both LG analogues and bound multi-group systems in the control sample, two-sample Kolmogorov-Smirnov tests comparing the distributions of gas content of LG analogues and the control sample show no significant difference in any crossing time bin. We conclude that the gas contents of LG analogues are very similar to the gas contents of other bound multi-group systems with similar mass.

Color Gap:

We calculate the color gap, as in Section 4.3.2, of LG analogues and the mass-matched control sample and compare the color gaps of the two types of systems over the range of system mass spanned by LG analogues. We find that the color gaps of LG analogues increase with system mass, whereas the color gaps of systems in the control sample decrease with system mass. The color gaps of LG analogues and systems in the control sample are statistically similar at higher system mass. Below the bimodality scale at a system mass of 10^{12} $M_\odot$, the distributions of color gap for LG analogues and groups in the mass-matched control sample differ by more than 3σ.

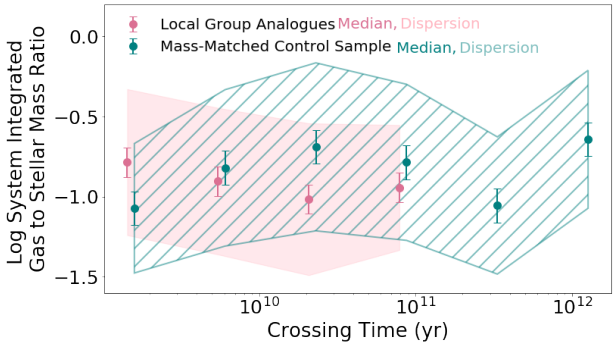

Figure 23: System integrated gas-to-stellar mass ratio vs. crossing time for LG analogues and the mass-matched control sample of non-LG analogue bound multi-group systems in ECO and RESOLVE-B. In each crossing time bin we plot the median and uncertainty in the median (as determined by smoothed bootstrapping). We also show the natural $\pm1\sigma$ spread in group gas content as shaded/hatched regions. The bin center crossing times of LG analogues are offset slightly towards lower crossing time to allow for easier visual comparison with the control sample.

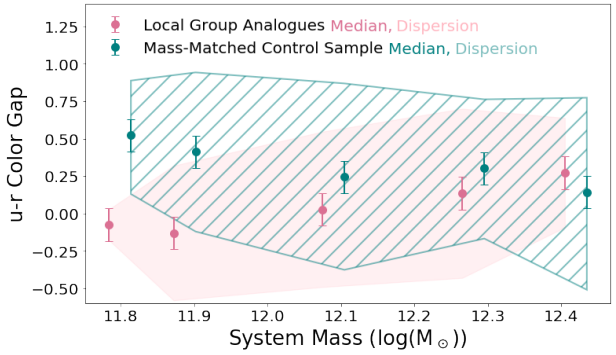

Figure 24: Color gap (as in Section 4.3.2) vs. system mass for LG analogues and the mass-matched control sample of non-LG analogue bound multi-group systems in ECO and RESOLVE-B. In each system mass bin we plot the median and uncertainty in the median (as determined by smoothed bootstrapping). We also show the natural $\pm1\sigma$ spread in group color gap as shaded/hatched regions. The bin center system masses of LG analogues are offset 0.03 dex towards lower system mass to allow for easier visual comparison with the control sample.

Figure 25 shows u-r color gap vs. crossing time for LG analogues and bound multi-group systems in the mass-matched control sample. The color gap of bound multi-group systems in the control sample mostly increases with crossing time (except in the longest crossing time bin). LG analogues show no clear trend in color gap

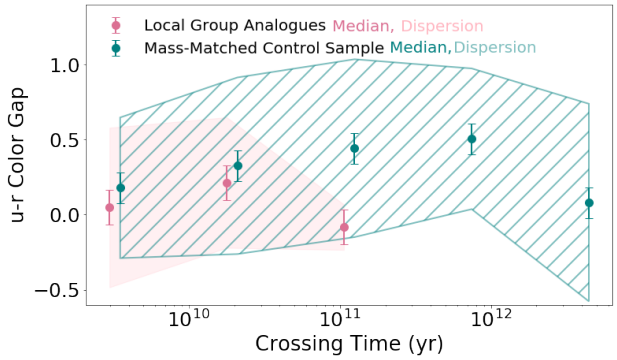

Figure 25: Color gap (as in Section 4.3.2) vs. crossing time for LG analogues and the mass-matched control sample of non-LG analogue bound multi-group systems in ECO and RESOLVE-B. In each crossing time bin we plot the median and uncertainty in the median (as determined by smoothed bootstrapping). We also show the natural $\pm1\sigma$ spread in group color gap as shaded/hatched regions. The bin center crossing times of LG analogues are offset slightly towards lower crossing time to allow for easier visual comparison with the control sample.

with crossing time. Two-sample Kolmogorov-Smirnov tests show no difference in the color gaps of LG analogues and bound multi-group systems in the control sample above 2σ significance in crossing time bins containing both types of systems. Although the color gaps of LG analogues differ from the color gaps of bound multi-group systems in the control sample at low system mass, the color gaps of the two types of systems do not differ significantly at fixed virialization state.

To better understand the differences in color gap between LG analogues and bound multi-group systems in the control sample, we compare distributions of the u-r colors of galaxies in LG analogues and bound multi-group systems in the control sample in each system mass bin used in Figure 24. These color distributions are shown in Figure 26. The bimodality in these distributions shows the blue and red sequences of galaxies. The color gaps of LG analogues differed most from the color gaps in the control sample in the two lowest system mass bins. Looking at the color distributions in these two bins, we see that in the control sample there are similar numbers of galaxies in the red and blue sequences, whereas for LG analogues one peak is much higher than the other (more blue galaxies in the lowest mass bin and more red galaxies in the second mass bin). These differences in the color distributions at low system mass lead to the differences in color gaps seen in Figure 24. The implications of these results for the evolutionary states of LG analogues remains an open question.

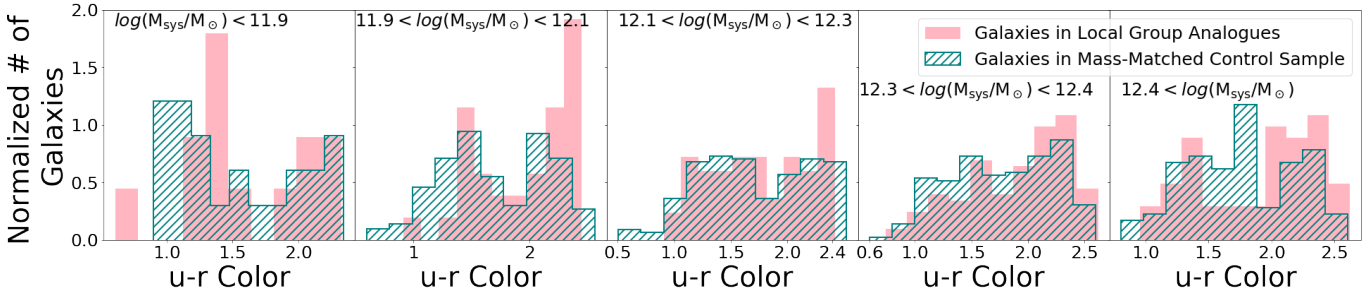

Figure 26: Distributions of u-r color for galaxies in both LG analogues and bound multi-group systems in the mass-matched control sample. Color distributions are broken into the same system mass bins used in Figure 24. Each distribution contains all of the galaxies that are members of systems that fall in the specified system mass range.

5. DISCUSSION

We compare our bound multi-group systems to the galaxy "associations" identified by Kourkchi & Tully (2017). Galaxy associations are systems that have decoupled from cosmic expansion, defined by the "surface of zero velocity" bounding a region that will eventually collapse. These associations are defined as containing all of the galaxies within the "first turnaround radius" (r_{1t}) which is a system mass-dependent radius that approximates the three-dimensional radius of the spherical surface of zero velocity. These galaxy associations, just like the bound multi-group systems that we identify, represent groups in the early stages of formation that have not yet collapsed into a settled group, but the method Kourkchi & Tully (2017) use to identify galaxy associations is complementary to the boundness method we use. Their method starts with a catalog of galaxies but does not use a group finder like FoF. Instead, they start with the most luminous galaxy in their sample and calculate the virial mass and first turnaround radius for that galaxy. They then add all galaxies within the first turnaround radius to the association and recalculate the mass and first turnaround radius for the association before adding galaxies within the new r_{1t}. This process continues until no new galaxies are added when r_{1t} is recomputed, at which point they move on to the next most luminous galaxy that is not already part of an association — and so on until every galaxy in the survey has been considered for membership in an association. Since membership in associations is dictated by whether the distance from the association center to a galaxy is less than the first turnaround radius of the association, the radius of a galaxy association is physically meaningful.

We compare the system radii of our bound multi-group systems to the mass-dependent first turnaround radii calculated by Kourkchi & Tully (2017) to determine whether most of our bound multi-group systems are likely decoupled from cosmic expansion. The catalog of galaxy associations from Kourkchi & Tully (2017) is publically available online, and includes the system mass and corresponding first turnaround radius of each galaxy association. The system radius of a bound multi-group system is the projection effect-corrected distance from the system center to the outermost galaxy in the bound multi-group systems. Figure 27 shows that bound multi-group system radii are grouped around the first turnaround radius for the system mass spanned by ECO and RESOLVE-B. About 84% of bound multi-group systems with system mass above $10^{12.5}$ $M_{\odot}$are contained within the first turnaround radius, and so are assumed to be decoupled from cosmic expansion. About 97.5% of bound multi-group systems with system mass above $10^{12.5}$ $M_{\odot}$are contained within two times the first turnaround radius. At lower system mass the median bound multi-group system radius is close to the first turnaround radius, meaning that about half of all bound multi-group systems with system mass less than about $10^{12.5}$ $M_{\odot}$lie outside of the first turnaround radius as calculated by Kourkchi & Tully (2017). About 97.5% of bound multi-group systems with system mass less than about $10^{12.5}$ $M_{\odot}$are contained within four times the first turnaround radius.

We found in Figure 12 that many proto-groups have crossing times much greater than the age of the Universe, meaning that no interaction would be expected between galaxies in these proto-groups in a meaningful length of time and these groups may not be contained within the first turnaround radius. We removed bound multi-group systems with crossing times greater than the age of the Universe from our comparison in Figure 27, shown in blue, and we see that for these crossing-time-limited bound multi-group systems the median system radius does stay within in the first turnaround radius for all system masses, indicating somewhat better agreement with Kourkchi & Tully (2017).

There are several possibilities for why we see so many bound multi-group systems with system mass less than about $10^{12.5}$ $M_{\odot}$that extend beyond the first turnaround

radius. Firstly, the boundness method does not take cosmic expansion into account when determining the relative velocity between groups, which could lead to our method overestimating the number of groups that are classified as gravitationally bound. There are also several factors that suggest uncertainty in the relation between system mass and first turnaround radius as calculated by Kourkchi & Tully (2017).

Kourkchi & Tully (2017) calculate the first turnaround radius from the total virial mass of the association using a relation found in Tully (2015). Because the first turnaround radius is very hard to determine observationally, Tully (2015) fit the relation between an association's virial mass and its first turnaround radius using only three associations. Additionally, the lowest mass association that was used in the fit is the Local Association (what we call the Local Group). The reason that many of our low system mass bound multi-group systems extend past the first turnaround radius may be due to uncertainty in the fit performed by Tully (2015), since very few associations were used in the fit for the first turnaround radius, and none of the associations has system mass below $\sim 10^{12}$ $M_{\odot}$.

Tully (2015) calculate the ratio of the first turnaround radius of associations to the "second turnaround radius" of groups (r_{2t}, very similar to the virial radius) at fixed system mass using empirical fits. They compare the ratio they calculate ($r_{1t}/r_{2t} = 3.14$) to the theoretically predicted ratio, which depends on the matter density of the Universe, Ω_m. They find that their calculated ratio implies a matter density of $\Omega_m = 0.15$, lower than the commonly accepted $\Omega_m = 0.3$, and they state that their empirical r_{1t}/r_{2t} ratio has large uncertainty. A larger ratio of r_{1t}/r_{2t} corresponds to a larger value of Ω_m, so it seems likely that the value of r_{1t}/r_{2t} from Tully (2015) is underestimated. This is consistent with the first turnaround radius being underestimated in (Kourkchi & Tully 2017), which would mean that more bound multi-group systems are truly contained within the first turnaround radius than are shown in Figure 27.

We compare the prevalence of bound multi-group systems whose constituent groups have overlapping virial radii to the prevalence of potentially merging groups identified in Tempel et al. (2017). Tempel et al. (2017) define potentially merging groups as nearby groups with on-sky projected separation is less than the sum of the groups' radii. Tempel et al. (2017) find 498 potentially merging groups out of 88,662 galaxy groups with at least two members in the SDSS main region, representing 0.6%. We find 116 groups with potentially interacting halos out of 4170 groups with two or more members in ECO, or about 2.8% (note that the smaller fraction of interacting halos here compared to Section 4.2.1 is because we exclude $N = 1$ groups here to match the method used in Tempel et al. 2017). One possible reason for our higher fraction of potentially interacting halos compared to Tempel et al. (2017) is our use of a volume-limited survey. Tempel et al. (2017) used the main region of SDSS, which is a flux-limited sample, and they observe that the frequency of merging groups varies with the groups' redshift (their Figure 1), with a higher frequency of merging groups found at lower redshift. Thus, their overall prevalence of 0.6% is likely artificially low because potentially merging groups are being missed at higher redshift in their flux-limited sample.

Leong & Saslaw (2004) examine the prevalence of groups like the Local Group whose low masses do not strongly perturb the Hubble flow beyond a radius of about 1.5 Mpc. They use a statistical mechanical approach to calculate the probability that a random configuration of N galaxies will be gravitationally bound. They find that at least 10% of galaxies should belong to a small gravitationally-bound group like the Local Group. We compare this prediction to the frequency of LG analogues we observe in our real data. In ECO, 8% of galaxies belong to a LG analogue, slightly less than the prediction by Leong & Saslaw (2004). However, Leong & Saslaw (2004) define their LG analogues as gravitationally bound systems with mass and separation similar to the LG and do not consider whether the system is isolated from nearby massive galaxies. Dropping the isolation constraint in our own LG analogue search to more closely match the criteria used in Leong & Saslaw (2004), we find that 15% of galaxies in ECO are members of bound multi-group systems with two giant galaxies that match the mass and separation constraints of the Local Group analogues, in agreement with the prediction of Leong & Saslaw (2004).

6. CONCLUSIONS

In this work, we present a new method that finds groups in early formation stages by testing for gravitational boundness between neighboring settled galaxy groups (groups that share a common dark matter halo, including $N = 1$ groups). We test for gravitational boundness between settled groups by comparing the escape velocity from one group at the location of the other to the relative velocity between the groups. We use mock catalogs of simulated 3D data to correct for projection effects in our calculations of escape velocities and relative velocities between groups. The boundness method is optimized for use in complete, volume- and absolute magnitude-limited samples, utilizing halo abundance matching to estimate halo mass from group-

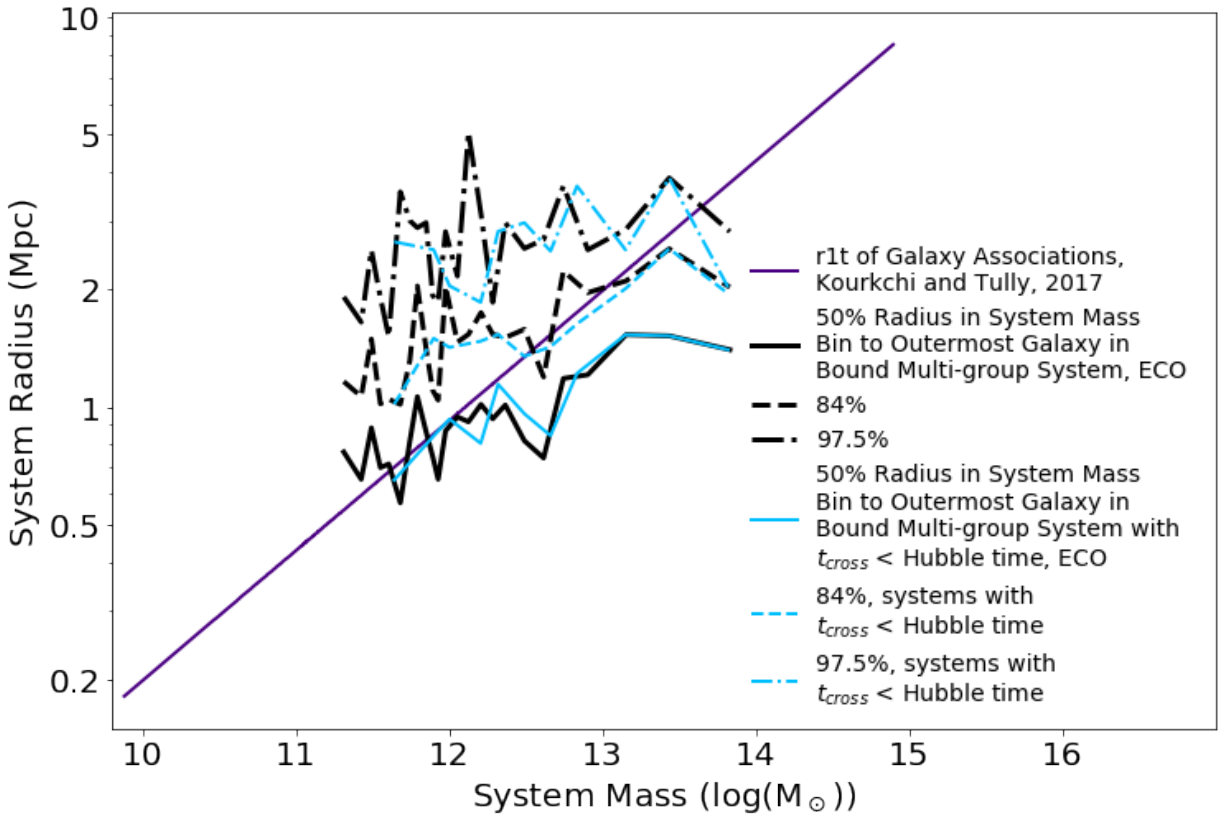

Figure 27: System radius vs. system mass for galaxy associations from Kourkchi & Tully (2017) and bound multi-group systems identified with the boundness method. For galaxy associations, the system radius is the first turnaround radius, or *r1t* calculated from system mass by Kourkchi & Tully (2017) and made publically available online. For bound multi-group systems, the system radius is the projection effect-corrected distance from the system center to the outermost galaxy in the bound multi-group system. The 50th, 84th, and 97.5th percentile system radius in each system mass bin is plotted for all bound multi-group systems in ECO in black, and for all bound multi-group systems with crossing time less than the age of the Universe in blue.

integrated luminosity. We use our boundness method to identify bound multi-group systems in RESOLVE and ECO, two volume-limited surveys of the local Universe. We use the bimodality mass scale of 10^{12} $M_\odot$to categorize groups and bound-multi-group systems by system mass. The bimodality scale is the halo mass at which halo gas is heated out to the virial radius of a group, preventing cold flows of gas that would otherwise fuel star formation from reaching the galaxy. Shock heating of halo gas begins at the center of a halo at the gas-richness threshhold halo mass scale of $10^{11.5} M_\odot$, which we define as the dwarf-giant divide (Dekel & Birnboim 2006; Kannappan et al. 2013). We use the method described in Section 3 to identify Local Group analogues in RESOLVE, ECO, and the mock catalogs.

- Testing for gravitational boundness reduces the number of $N = 1$ groups and increases the number of multiple galaxy systems in RESOLVE and ECO. There is a corresponding decrease in the number of low mass systems ($M_{\rm system} < 10^{11.5} M_\odot$) and an increase in giant systems (Figure 9). Approximately 20% of all galaxies in ECO are members of a bound multi-group system.

- We identify 32 Local Group (LG) analogues in RESOLVE and 229 in ECO, comprising about 13% of all multiple-member galaxy systems. About 8% of all galaxies in RESOLVE and ECO belong to a LG analogue.

- We find evidence that confirms that the boundness method succeeds at finding groups in the early stages of formation.

    1. We find that 18% of bound multi-group systems in RESOLVE and 22% in ECO contain FoF groups with overlapping virial radii, suggesting that the halos may be interacting.

2. Tests of virialization state indicate that bound multi-group systems are less virialized than settled groups (Figures 11 and 12).
3. Proto-groups (bound multi-group systems with system mass below the bimodality scale) and small settled groups (settled groups with halo mass below the bimodality scale) are found in the same large-scale environments (Figure 13), possibly making an evolutionary connection between the two types of groups possible.

- Using mock catalogs, we assess the purity and completeness of our bound multi-group systems and LG analogues, and test how effectively the boundness method identifies LG analogues.
  1. We find high completeness (90%) and high purity (86%) of bound multi-group systems identified with 2D data compared to the true bound multi-group systems identified with 3D data.
  2. We find high completeness (89%) but lower purity (73%) of LG analogues identified with 2D data compared to the true LG analogues identified with 3D data.
  3. The boundness method applied to the mock catalogs using 2D data identifies 97% of true LG analogues (identified using 3D data) as part of a common bound multi-group system, confirming that the boundness method succeeds in identifying groups like the Local Group.
- We use gas content and "color gap" (the difference in u-r color between the brightest and second brightest galaxy in a system) to compare the evolutionary states of different groups and systems as a function of system mass and crossing time.
  1. We find no statistically significant difference in the distributions of gas content or color gap for proto-groups and small settled groups as a function of system mass (Figures 14 and 17). Small settled groups have higher gas content than proto-groups at fixed group crossing time at 2-3σ confidence (Figure 15).
  2. We find no statistically significant difference in the distributions of gas content for LG analogues and a mass-matched control sample of bound multi-group systems (Figures 22 and 23). The color gaps of LG analogues are smaller than those of systems in the control sample at more than 3σ significance below a system mass of 10^{12} $M_{\odot}$(Figure 24).
- LG analogues are among the most virialized bound multi-group systems according to a comparison of crossing times with systems in a mass-matched control sample (Figure 20). LG analogues contain FoF groups with overlapping halos at about the same frequency as systems in the mass-matched control sample.
- LG analogues are more commonly found in less dense large-scale environments than systems in the mass-matched control sample (Figure 21).
- The fraction of galaxies in ECO that belong to a LG analogue agrees with predictions made by Leong & Saslaw (2004) when the same set of criteria they used in simulations are adopted in ECO.
- Most bound multi-group systems with system mass above about $10^{12.5}$ $M_{\odot}$are decoupled from cosmic expansion according to the method from Kourkchi & Tully (2017). Many lower mass bound multi-group systems are not decoupled from cosmic expansion according this method, possibly because the method is calibrated using only three systems, all with high system mass.
- Our volume-limited analysis reveals a higher fraction of potentially merging groups by a factor of 4.5 than compared to the flux-limited analysis of Tempel et al. (2017).

Expanding our inventory of multi-galaxy systems to include bound multi-group systems as well as settled groups will allow us to study how galaxy groups form and evolve and what role merging into a common dark matter halo may play, e.g. due to shock heating of halo gas at critical mass scales.

In this paper, we have taken the first steps by applying our boundness and Local Group analogue criteria to surveys in the local Universe. In ECO, 7% of galaxies that reside in their own halo (and thus their own settled group) are actually bound in a proto-group, and 8% of all galaxies in ECO are members of a LG analogue. This work sets the stage for further comparative analysis of galaxy evolution across these new environmental categories as well as cosmic time.

7. ACKNOWLEDGEMENTS

I would like to thank my advisor Sheila Kannappan for all of her support, help, advice, and ideas throughout my project. I would also like to thank Zackary

Hutchens for his mentorship and help. I also thank other collaborators Andreas Berlind, Kathleen Eckert, Victor Calderon, Mehnaaz Asad, Darren Croton, and the RESOLVE team. Finally, I thank Adrienne Erickcek for her helpful comments.

REFERENCES

Abadi, M. G., Moore, B., & Bower, R. G. 1999, Monthly Notices of the Royal Astronomical Society, 308, 947

Bentley, J. L. 1975, Communications of the Association for Computing Machinery, 18

Berlind, A. A., Frieman, J., Weinberg, D. H., et al. 2006, The Astrophysical Journal Supplement Series, 167, 1

Blanton, M. R., & Berlind, A. A. 2007, The Astrophysical Journal, 664, 791

Bryan, G. L., & Norman, M. L. 1998, The Astrophysical Journal, 495, 80

Carlesi, E., Yehuda, H., Gottlober, S., et al. 2019, Monthly Notices of the Royal Astronomical Society, 491, 1531

Carollo, C. M., Cibinel, A., Lilly, S. J., et al. 2013, The Astrophysical Journal, 776, 38

Cox, T., & Loeb, A. 2008, Monthly Notices of the Royal Astronomical Society, 386, 461

Dekel, A., & Birnboim, Y. 2006, Monthly notices of the royal astronomical society, 368, 2

Dressler, A., & Shectman, S. A. 1988, The Astronomical Journal, 95, 985

Duarte, M., & Mamon, G. A. 2014, MNRAS, 440, 1763, doi: 10.1093/mnras/stu378

Eckert, K. D., Kannappan, S. J., Stark, D. V., et al. 2016, The Astrophysical Journal, 824, 124

—. 2015, The Astrophysical Journal, 810, 166

Eckert, K. D., Kannappan, S. J., Lagos, C. d. P., et al. 2017, The Astrophysical Journal, 849, 20

Fattahi, A., Navarro, J. F., Sawala, T., et al. 2016, Monthly Notices of the Royal Astronomical Society, 457, 844

Ferguson, H. C., & Sandage, A. 1990, The Astronomical Journal, 100

Firth, P., Evstigneeva, E., Jones, J., et al. 2006, Monthly Notices of the Royal Astronomical Society, 372, 1856

Gade, K. 2010, The Journal of Navigation, 63, 395

Garrison-Kimmel, S., Hopkins, P. F., Wetzel, A., et al. 2019, Monthly Notices of the Royal Astronomical Society, 487, 1380

Gunn, James E., G. J. R. I. 1972, The Astrophysical Journal, 196

Hodges, J. L. 1958, Arkiv för Matematik, 3, 469

Hou, A., Parker, L. C., Harris, W. E., & Wilman, D. J. 2009, The Astrophysical Journal, 702, 1199

Hu, W., & Kravtsov, A. V. 2003, The Astrophysical Journal, 584, 702

Huchra, J., & Geller, M. 1982, The Astrophysical Journal, 257, 423

Joseph, R. D., & Wright, G. S. 1985, Monthly Notices of the Royal Astronomical Society: Letters, 214, 87

Kannappan, S. J., & Wei, L. H. 2008, AIP Conference Proceedings, 1035, 163

Kannappan, S. J., Stark, D. V., Eckert, K. D., et al. 2013, The Astrophysical Journal, 777, 42

Kourkchi, E., & Tully, R. B. 2017, The Astrophysical Journal, 843, 16

Larson, R. B., Tinsley, B. M., & Caldwell, C. N. 1980, The Astrophysical Journal, 237, 15

Leong, B., & Saslaw, W. C. 2004, The Astrophysical Journal, 608, 636

Li, Y.-S., & White, S. D. M. 2008, Monthly Notices of the Royal Astronomical Society, 384, 1459

Moffett, A. J., Kannappan, S. J., Berlind, A. A., et al. 2015, The Astrophysical Journal, 812, 89

Old, L., Skibba, R. A., Pearce, F. R., et al. 2014, Monthly Notices of the Royal Astronomical Society, 441, 1513

Rasmussen, J., Bai, X.-N., Mulchaey, J. S., et al. 2012, The Astrophysical Journal, 747, 14

Rood, H. J., & Dickel, J. R. 1978, The Astrophysical Journal, 224, 724

Spekkens, K., Urbancic, N., Mason, B. S., Willman, B., & Aguirre, J. E. 2014, The Astrophysical Journal, 795, 4

Stark, D. V., Kannappan, S. J., Eckert, K. D., et al. 2016, The Astrophysical Journal, 832, 126

Stothert, L., Norberg, P., & Baugh, C. 2019, Monthly Notices of the Royal Astronomical Society: Letters, 485, L126

Tempel, E., Tuvikene, T., Kipper, R., & Libeskind, N. I. 2017, Astronomy & Astrophysics, 602, A100

Tully, R. B. 2015, The Astronomical Journal, 149, 18

van der Marel, R. P., Besla, G., Cox, T., Sohn, S. T., & Anderson, J. 2012, The Astrophysical Journal, 753, 21

Wang, S. 1995, Annals of the Institute of Statistical Mathematics, 47, 65

Zhai, M., Guo, Q., Zhao, G., Gu, Q., & Liu, A. 2020, The Astrophysical Journal, 890, 27